

Collaborative Continuum Robots: A Survey

Xinyu Li, *Student Member, IEEE*, Qian Tang, Guoxin Yin, Gang Zheng, *Senior Member, IEEE*, Jessica Burgner-Kahrs, *Senior Member, IEEE*, Cesare Stefanini, *Member, IEEE*, Ke Wu, *Member, IEEE*

Abstract—Continuum robots (CRs), owing to their compact structure, inherent compliance, and flexible deformation, have been widely applied in various fields. By coordinating multiple CRs to form collaborative continuum robots (CCRs), task adaptability, workspace, flexibility, load capacity, and operational stability can be further improved, thus offering significant advantages. In recent years, interest in this emerging field has grown steadily within the continuum-robotics community, accompanied by a consistent rise in related publications. By presenting a comprehensive overview of recent progress from different system-architecture levels, this survey provides a clear framework for research on CCRs. First, CCRs are classified into the three collaboration modes of separated collaboration, assistance collaboration, and parallel collaboration, with definitions provided. Next, advances in structural design, modeling, motion planning, and control for each mode are systematically summarized. Finally, current challenges and future opportunities for CCRs are discussed.

Index Terms—Collaborative continuum robots, structural design, modeling, motion planning, control.

I. INTRODUCTION

CONTINUUM Robots (CRs), inspired by flexible structures in nature, are characterized by an actuation system decoupled from the deformable body, while maintaining tangent continuity along the backbone during deformation [1], [2]. This design provides CRs with a compact structure, inherent compliance, and flexible deformation, enabling effective operation in regions inaccessible to rigid robots [3]. Consequently, CRs have found widespread applications in minimally invasive surgery [4], equipment repair [5], and underwater operations [6].

Despite the increasing deployment of CRs in practical applications, several critical limitations remain. Tasks such as knotting [7], gripping [8], and locomotion [9] often exceed the capability of a single CR, constraining task adaptability. Moreover, their high compliance makes them prone to deformation under external loads [10]. Therefore, it is imperative to extend the traditional design paradigm of CRs by enabling multiple CRs to collaborate, thereby forming multi-arm collaborative continuum robots (CCRs) that offer new opportunities for accomplishing complex tasks.

The concept of “multi-arm collaboration” was initially introduced in industrial robotics [11]. To address the high-DOF requirements of complex tasks, collaborative robots have progressed from fully actuated rigid systems with few DOFs [12], [13], to partially actuated systems with moderate DOFs [14], [15], and ultimately to underactuated CCRs offering theoretically infinite DOFs [16], [17], as illustrated in Fig. 1. In this process, the collaboration paradigm has evolved from discrete, joint-based coordination to continuous, deformation-driven

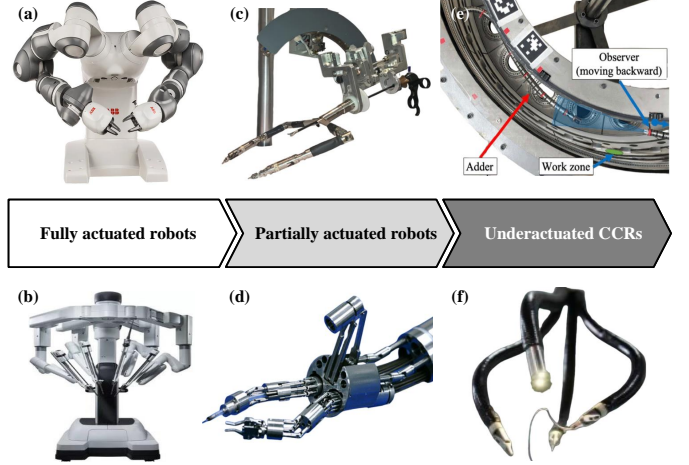


Fig. 1. Development of representative collaborative robots. (a) YuMi dual-arm robot [13]. (b) Da Vinci surgical robot [12]. (c) The Hong Kong Polytechnic University R&D surgical robot [14]. (d) Waseda University R&D surgical robot [15]. (e) University of Nottingham R&D repair CCR [16]. (f) Shanghai Jiao Tong University R&D surgical CCR [17].

coupling. Consequently, the coupling relationships among CRs have become a central focus in CCRs research. CCRs are herein classified into three modes, namely separated collaboration, assistance collaboration, and parallel collaboration. Separated collaboration decomposes complex tasks that are difficult for a single CR into simpler subtasks executed cooperatively by multiple CRs, thereby improving adaptability in complex tasks [18] (Figs. 2(a)–2(j)). Assistance collaboration physically links CRs to support the master arm, extending its workspace and flexibility [19], [20] (Figs. 2(k)–2(p)). Parallel collaboration attaches the end-effectors of multiple CRs to a common mobile platform, forming a parallel configuration that enhances load capacity and operational stability while maintaining overall compliance [21] (Fig. 2(q)–2(u)). Research on these CCRs is typically based on single-CR frameworks and considering interactions between multiple CRs or between CRs and the environment at different system architecture levels (structural, modeling, motion planning, and control), as shown in Fig. 2(v).

Several existing reviews (Table I) have also discussed aspects of CCR in specific contexts. For example, Ref. [37] introduced the structural design of CRs in medical surgery scenarios, and [38] and [39] further explored their modeling, motion planning and control strategies, some of which can be categorized as separated collaboration in CCR. [40] discussed the structural design and modeling of parallel continuum robots (PCRs), while [41] subsequently classified PCRs into

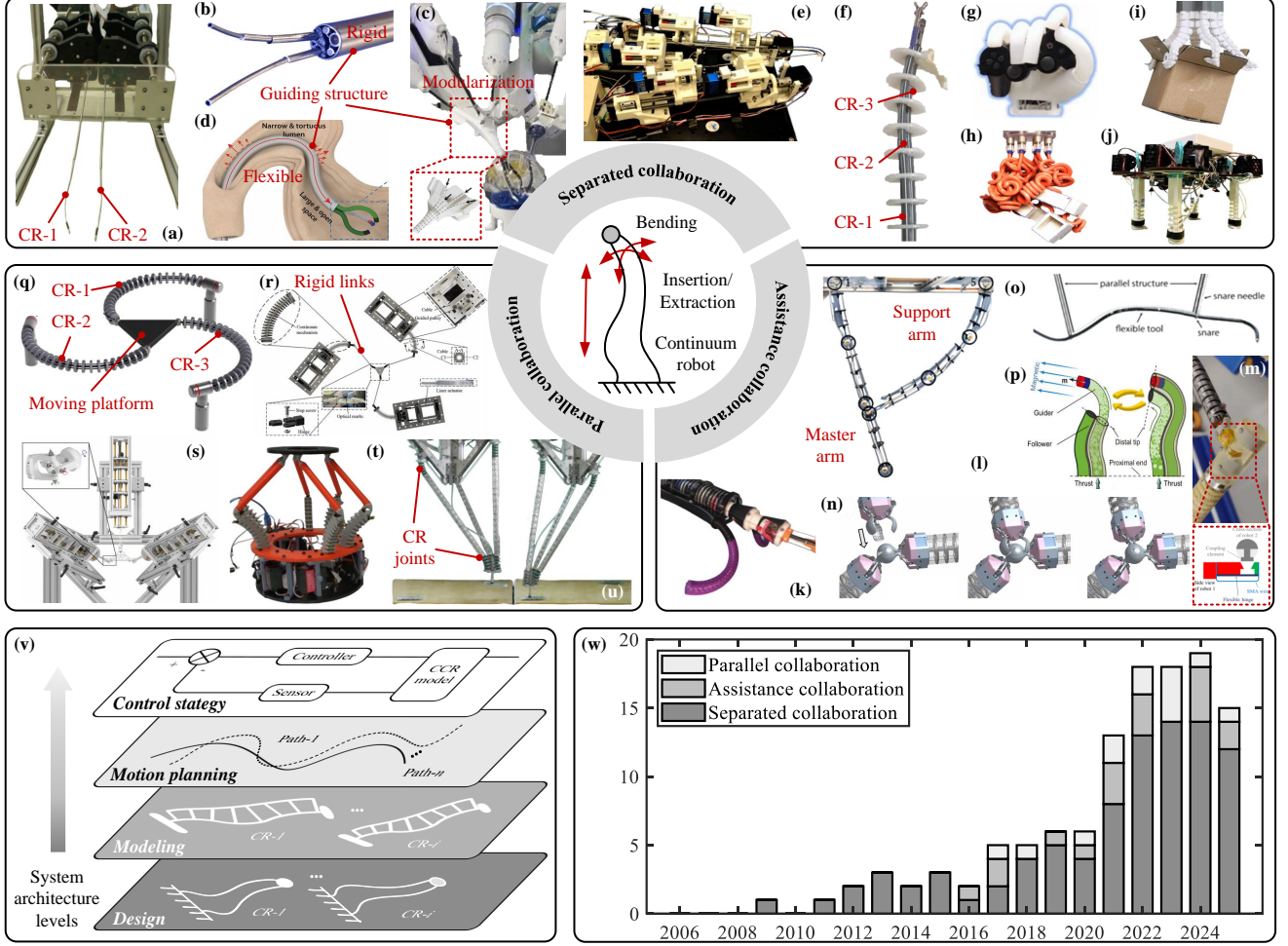


Fig. 2. Classification and representative examples of CCRs. (a) Dual-arm concentric tube robots [18]. (b) Rigid guiding structures [22]. (c) Modular guiding structures [17]. (d) Flexible guiding structures [23]. (e) Pyramid-type actuation [24]. (f) Without flexible guiding structures [25]. (g) Dexterous hand [26]. (h) Multiple fluid-driven CRs [27]. (i) Logarithmic spiral-based structure [28]. (j) CCR-based legged robot [29]. (k) Inspired by Angel Oak tree growth [20]. (l) Multi-port design [30]. (m) Shape-memory alloy connectors [31]. (n) Multi-finger spherical gripper [32]. (o) Reconfigurable design [19]. (p) Alternating follower motion [33]. (q) Planar configuration with CRs [34]. (r) Planar configuration with CRs and rigid links [21]. (s) Spatial configuration with CRs [35]. (t) Spatial configuration with high load capacity [10]. (u) Composed of CR joints [36]. (v) System architecture levels of CCRs. (w) Publication statistics on CCR-related studies.

active and passive types, with some active forms considered parallel collaborative. [42], [43], [44], [45], and [46] reviewed grasper and dexterous-hand structures composed of multiple CRs, while [47] reported on biomimetic soft-legged robots driven by multiple CRs, addressing aspects of structural design, modeling, and control strategies. Several of these designs can also be categorized as separated collaborative. However, these reviews lack a clear definition, a classification, and a comprehensive analysis of CCR, which prevents readers from fully understanding its evolution and key challenges. Therefore, a systematic survey of CCR is urgently needed.

The keyword “collaborative continuum robot” was searched in the Web of Science and Scopus databases, and the results were filtered to identify publications relevant to this field. The analysis reveals a steady increase in research activity within the CCR field, with separated collaboration remaining the dominant focus, while studies on assistance collaborative and parallel collaborative have also grown consistently in recent years, as depicted in Fig. 2(w). These findings indicate that

CCR research is still at a critical stage of development, particularly suggesting significant opportunities for future exploration in assistance collaborative and parallel collaborative areas. The main contributions of this survey are summarized as follows:

- 1) To the best of our knowledge, this is the first systematic survey focusing on CCRs.
- 2) The collaborative modes of CCRs are classified, followed by a comprehensive survey of current research on structural design, modeling, motion planning, and control.
- 3) The current challenges and future opportunities are identified to support the further development of CCRs.

The rest of this survey is organized as follows. Section II defines the three collaborative modes of CCRs and introduces their structural designs. Section III summarizes two modeling strategies of CCRs and further discusses the formulation of coupling constraints. Section IV reviews motion planning methods and control strategies for CCRs. Section V discusses current challenges and future opportunities. Finally, Section

TABLE I
SUMMARY OF RELATED REVIEWS FOR CCRs

Ref.	Year	Review Title	Contents Related to CCRs	Application	Relevance to CCR
[38]	2018	Medical technologies and challenges of robot-assisted minimally invasive intervention and diagnostics	SC: S-M-C	Surgery	H
[42]	2020	In the soft grip of nature	SC: S	Grasping	L
[37]	2021	Research progress and development trend of surgical robot and surgical instrument arm	SC: S	Surgery	M
[39]	2022	Continuum robots for endoscopic sinus surgery: Recent advances, challenges, and prospects	SC: S-P-C	Surgery	H
[43]	2023	Current designs of robotic arm grippers: A comprehensive systematic review	SC: S	Grasping	L
[41]	2024	Parallel-continuum robots: a survey	PC: S-M	–	M
[40]	2024	Design, modeling, and evaluation of parallel continuum robots: a survey	PC: S-M-O	–	M
[47]	2024	Biomimetic soft-legged robotic locomotion, interactions and transitions in terrestrial, aquatic and multiple environments	SC: S-M-C	Locomotion	H
[44]	2024	Actuated Palms for Soft Robotic Hands: Review and Perspectives	SC: S	–	L
[45]	2024	Variable stiffness soft robotic gripper: design, development, and prospects	SC: S	–	L
[46]	2025	Dexterous hand towards intelligent manufacturing: A review of technologies, trends, and potential applications	SC: S	–	L

SC: Separated Collaboration; AC: Assistance Collaboration; PC: Parallel Collaboration

S: Structure Design; M: Modeling; P: Motion Planning; C: Control Strategy; O: Other Contents

H: High; M: Medium; L: Low (determined by the number of related publications involving CCRs)

VI concludes the survey.

II. STRUCTURE DESIGN OF CCRs

The structural design of CCRs serves as the foundation for their performance and functional implementation. Unlike single CRs, CCRs require the additional design of multiple CRs' configuration layouts and interconnections to meet specific task requirements [30]. In this section, three representative collaboration modes are defined, and their structural forms are presented and analyzed. Table II further compares these modes in terms of their actuation mechanisms, advantages, limitations, and application scenarios.

A. Separated collaboration

In the separated collaboration mode, n ($n \geq 2$) CRs without mechanical linkage operate autonomously yet in coordination, thereby enabling tasks beyond the capability of a single CR. Task-specific actuation mechanisms can be selected according to mission characteristics, as shown in Table II.

In this collaboration mode, the typical structural design can be described as a direct composition of multiple CRs (Fig. 2(a)) [18], [48]. With the evolution of CCRs, equipping individual CR end-effectors with different tools provides the system with the capability to perform multiple tasks, such as cutting [49]–[52], suturing [53], and repairing [16].

As with single CRs, enhancing the task-execution performance of individual CRs within a CCR remains an active research topic. By incorporating rigid guiding structures with axial channels (Fig. 2(b)), multiple CRs can be directed to distal regions, thereby expanding the workspace in confined environments [22], [54]. Furthermore, a modular guiding structure design with replaceable CRs (Fig. 2(c)) [17], [55] improves the versatility and maintainability of the CCR. When the target path contains frequent bends, the guiding structure can instead be designed as a flexible CR (Fig. 2(d)), increasing the CCR's dexterity [23], [52], [56]. On

this basis, the structural parameters of the CCR body can be optimized using algorithms such as particle swarm optimization [57], the Nelder–Mead simplex algorithm [48], and the adaptive parameter grey wolf–cuckoo search algorithm [52], thus improving collaborative performance. Furthermore, the load-bearing capacity of CCRs can be effectively improved through rolling-joint designs and redundant-DOF constraint mechanisms [51], [58], external locking cables [59], or variable-stiffness structures based on granular and layer jamming techniques [60]. To further mitigate inter-segment coupling effects, hybrid rigid–flexible structures [61], [62] and mixed actuation schemes [63] have been explored. However, these improvements inevitably increase the overall size and complexity of CCRs, introducing collision risks. To address this issue, one approach is to adjust the angular arrangement of CRs [64] and the pose of the base [17] to prevent collisions among CRs. Another approach is to employ a pyramid-type actuation structure (Fig. 2(e)) [24], [55], where multi-objective optimization is applied to its design parameters [65], [66] to avoid internal interference among components. Moreover, exploiting shape-coupling interactions among CRs enables indirect control of flexible guiding structures (Fig. 2(f)) [25], [67], thereby eliminating the need for dedicated actuators and reducing both system complexity and the overall size of the CCR.

In this collaboration mode, another active research focus is object grasping [6], [8]. In such cases, individual CRs are anchored to the same or different mobile/fixed bases and grasp the target object through synchronized deformation [68], [69]. In recent years, diverse structural forms have been developed, including variable-stiffness tendon-driven structures based on layer jamming [70], actuators composed of magnetically programmable soft materials [71], [72], and pneumatic artificial muscle–driven structures [6], [73], [74]. Integrated assemblies of these structures can further constitute CCRs [9], [75]–[77]. In addition, dexterous hands composed of CR-based fingers (Fig. 2(g)), which commonly adopt tendon-driven [78], pneu-

TABLE II
COMPARISON OF COLLABORATIVE MODES FOR CCRs

Mode	Ref.	Actuation	Application	Advantages	Limitations
SC	[9], [18], [22], [25], [48], [50], [52], [53], [54], [55], [57], [67]	Concentric tube	SU		
	[16], [17], [28], [29], [49], [51], [52], [58], [59], [62], [64], [78]	Tendon	SU-MA-GR-LO	(1) Facilitates modular integration, enabling rapid deployment and maintenance. (2) High scalability and adaptability support flexible task execution.	(1) Limited load capacity due to lack of physical interconnection. (2) Coordinated performance strongly depends on perception accuracy.
	[56], [61], [79]	Rod	SU		
	[6], [27], [73], [74], [78], [86], [95]	Pneumatic	GR-LO		
	[81]	Hydraulic	GR		
	[82], [94]	Origami	GR		
	[23], [26], [60], [63], [70], [96]	Hybrid	SU-GR-LO		
AC	[10], [20], [30], [32], [99], [112]	Tendon	SU-MA-LO	(1) Flexible support allows task-specific reconfiguration. (2) Improves payload capacity and long-reach operation.	(1) Coupling structures increase system complexity. (2) High coordination is required for stable control.
	[33], [101]	Magnetic	SU		
	[31]	Hybrid	MA		
PC	[11], [21], [34], [35], [36], [106], [107]	Tendon	SU-MA	(1) Significantly enhances system stiffness and stability. (2) Offers high precision in pose control with responsive manipulation.	(1) Complex constraints limit flexibility and workspace. (2) Modeling and coordinated control are highly complex.

SC: Separated Collaboration; AC: Assistance Collaboration; PC: Parallel Collaboration

SU: Surgery; MA: Maintenance; GR: Grasping; LO: Locomotion

matic [79], [80], hydraulic [81], dielectric-elastomer-based [75], origami-inspired [82], or hybrid actuation schemes [26], can also be regarded as a form of separated collaboration. Structural optimization has further been shown to enlarge their workspace [83] and improve grasping performance [84]. However, in most dexterous hands, each finger mimics human anatomy through a finite number of discrete joints, placing them outside the scope of this survey. Comprehensive reviews are available in [44]–[46].

The extensive application of bionics has significantly advanced grasping capabilities. By mimicking the coiling and entangling functions of octopus tentacles, elephant trunks, and plants [27], [85], CRs can achieve complex object grasping. For instance, the design of multiple fluid-driven CRs enables stochastic-topology grasping (Fig. 2(h)), thereby eliminating the need for sophisticated perception and feedback strategies during the grasping process [27]. Further, incorporating hard bulges on the CR surface allows for diverse grasping strategies [86], while tendon-driven logarithmic spiral-shaped simplified structures (Fig. 2(i)) improve controllability in grasping tasks [28]. In addition, mounting CCRs on mobile bases such as unmanned aerial vehicles [86], [87], automated guided vehicles [88], industrial robots [89]–[91], or CCR-based legged robots (Fig. 2(j)) [9], [29], [92]–[98] can substantially expand their task adaptability.

B. Assistance collaboration

The assistance collaboration mode of CCRs refers to a configuration in which n ($n \geq 2$) CRs cooperate with unequal roles to accomplish a task. In this mode, one or more CRs act as support arms, with their ends connected to the side of the master CR. These support arms provide support to the master arm, assisting it in accomplishing the target task [99].

An interesting design inspired by the growth pattern of the Angel Oak Tree proposes a tendon-driven concentric-tube structure featuring lateral branches. In this configuration, as the master arm extends continuously, support arms extend laterally to support its motion (Fig. 2(k)) [20]. Although this approach enhances the stiffness of the main arm, it faces limitations in maneuverability within confined spaces. To improve adaptability, multi-portal CCR configurations can be developed, allowing small-diameter master and support arms to enter through different access points and achieve connections in the target area (Fig. 2(l)) [99]. Based on this structure, the stiffness of the master arm can be tuned by varying the position and angle of the connection points [30], [100]. In addition, connection devices based on shape memory alloys can be introduced to enable rapid connection and disconnection through temperature changes [31], thereby simplifying the connection process and enhancing the mechanical reliability at the connection sites (Fig. 2(m)). To improve multi-directional adaptability of the connection devices, multi-fingered spherical grippers with open-close functionality can also be employed (Fig. 2(n)) [32].

When performing narrow-path navigation tasks, to control the size of the driving device while ensuring sufficient degrees of freedom (DOFs), a slender master arm that can pass through a smaller entrance may be used. On this basis, a series of support arms can be inserted at points along the path of the main arm and fixedly connected to its side, thereby reconstructing the starting point of the master arm and improving its flexibility without increasing the overall size of the CR (Fig. 2(o)) [19]. In addition, a magnetically actuated parallel casing structure can be employed, in which individual casings alternately harden and soften to enable alternating follower motion (Fig. 2(p)) [33], [101].

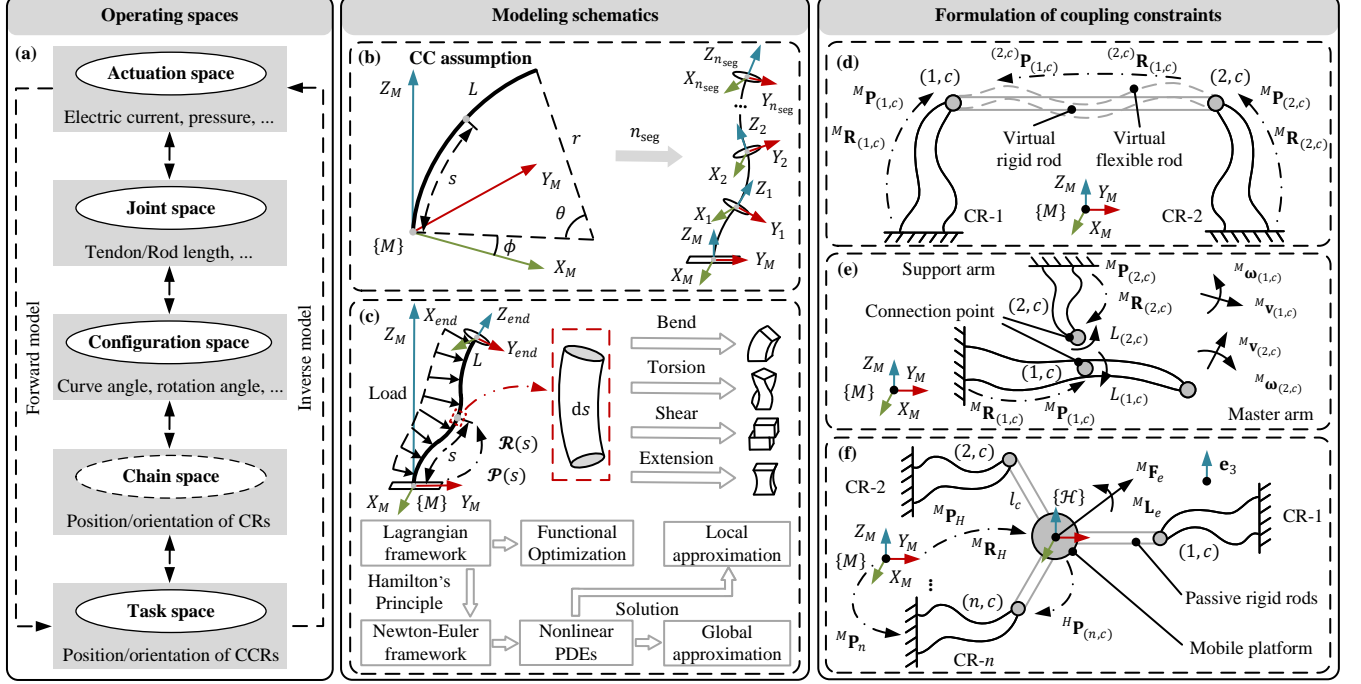


Fig. 3. Coupling modeling strategies for CCRs. (a) Operating spaces of coupling modeling strategies. (b) Schematic of the PCC model. (c) Schematic of the Cosserat rod theory. (d) Formulation of coupling constraints for separated collaboration. (e) Formulation of coupling constraints for assistance collaboration. (f) Formulation of coupling constraints for parallel collaboration.

C. Parallel collaboration

The parallel collaboration mode of CCRs refers to a configuration in which n ($n \geq 3$) CRs with equal roles are symmetrically arranged in a circular arrangement, with their ends connected to a shared moving platform that serves as the end-effector of the CCR, thereby enabling high-precision and high-load tasks.

PCRs constructed using rods arranged in parallel [102], [103], compliant joints [104], or pneumatic chambers [105] as actuation elements can be considered the earliest form of the parallel collaborative configuration, with comprehensive summaries available in Refs. [40] and [41]. However, these actuation elements rely solely on passive deformation through axial extension or contraction under material constraints, essentially remaining within the scope of single CRs. To further enhance motion capabilities and stiffness characteristics, parallel collaborative configurations composed of CRs with active deformation capability have been proposed [36].

Currently, representative studies focus on planar configurations either consisting of three tendon-driven CRs (Fig. 2(q)) or comprising three CRs combined with passive rigid links (Fig. 2(r)). The individual components are interconnected via spherical joints, enabling the moving platform to achieve 3 DOFs (\vec{x} , \vec{y} , and \vec{z}), with high repeatability [21], [34], [106]. By optimizing the parameters of the CRs, passive rigid links, and actuation layouts, the workspace size and shape can be adjusted to achieve optimal configurations tailored for specific applications [107]. Transitioning from planar to spatial arrangements of CRs increases the moving platform's DOFs to 6 (\vec{x} , \vec{y} , \vec{z} , \tilde{x} , \tilde{y} , and \tilde{z}), thereby enhancing its motion capabilities (Fig. 2(s)) [35]. Moreover, increasing the number

of parallel CRs to 6 can significantly improve the load-bearing capacity of the moving platform (Fig. 2(t)) [10]. Additionally, another approach to parallel collaboration retains rigid links but replaces the joints at both ends with CRs. Compared to traditional spherical joints, this design avoids potential damage to precision workpieces while maintaining high positioning accuracy (Fig. 2(u)) [36].

D. Summary

Across the three collaboration modes, the structural evolution of CCRs consistently reflects a pursuit of enhanced task-execution performance. In the separate mode, structurally independent CCRs are evolving stronger cooperative capability. However, trade-offs remain between performance-driven structural complexity and collision-free multi-CR design. In the assistance mode, the supporting CRs is mechanically coupled to the master CR and is transitioning from fixed to reconfigurable coupling configurations to improve operability in complex environments, yet existing studies insufficiently address the structural trade-offs among load-bearing capacity, actuation complexity, and response speed. In the parallel mode, multiple CRs are coupled at their ends to accomplish tasks collectively, with structures shifting from planar to spatial parallel architectures and incorporating more CRs to enhance overall output performance. However, the resulting increase in multi-CR coupling complexity introduces stringent requirements on dimensional controllability and assembly quality.

III. MODELING OF CCRs

Building on the coupled structural design of CCRs, a mathematical model needs to be developed through parameterized

TABLE III
COMPARISON OF MODELING METHODS FOR CCRs

Ref.	Mode	Modeling methods	Constraint types	IK solution	Position error	Orientation error	Model type
[49]	SC	PCC	—	Numerical	2.500 mm (0.463%)	—	Kinematic
[64]	SC	PCC	—	—	0.700 mm (0.538%)	—	Kinematic
[52]	SC	CC	—	Numerical	—	—	Kinematic
[69]	SC	PCC	GC	Numerical	1.000 mm~2.000 mm (0.333%~0.667%)	—	Kinematic
[7]	SC	PCC	—	Numerical	1.600 mm~2.100 mm (0.425%~0.525%)	—	Kinematic
[119]	SC	CC	GC	Analytical	1.200%	—	Kinematic
[67]	SC	Cosserat rod	GC-FC	—	3.560%	—	Kinostatic
[25]	SC	Cosserat rod	GC-FC	Numerical	1.960 mm (2.800%)	6.700°	Kinostatic
[30]	AC	Cosserat rod	GC-VC	—	2.900%	—	Dynamic
[19]	AC	Cosserat rod	GC-FC	Numerical	3.680 mm (0.775%)	—	Kinostatic
[111]	AC	Cosserat rod	GC-FC	Numerical	1.800 mm (0.180%)	5.600°	Kinostatic
[99]	AC	CC-Cosserat rod	GC-FC	Numerical	—	—	Kinostatic
[112]	AC	Cosserat rod	GC-FC-VC	—	3.950%	—	Dynamic
[107]	PC	CC	GC	Numerical	1.400%	1.100°	Kinematic
[106]	PC	CC	GC	Numerical	—	—	Kinematic
[21]	PC	CC	GC	Numerical	0.900 mm~1.400 mm	—	Kinematic
[113]	PC	Cosserat rod	GC-FC	Numerical	4.900 mm (3.379%)	6.200°	Kinostatic

SC: Separated Collaboration; AC: Assistance Collaboration; PC: Parallel Collaboration

GC: Geometric Constraints; FC: Force/Moment Constraints; VC: Speed Constraints

structural features to incorporate kinematic states and mechanical coupling constraints among n CRs, thereby ensuring coordinated motion of the CCR. In this section, two common modeling strategies for CCRs are introduced, followed by a description and summary of the methods for formulating coupling constraints in three representative collaboration modes.

A. Modeling strategies

Due to the structural complexity of CCRs, two modeling strategies are commonly employed, which include independent modeling and coupled modeling. In the independent modeling strategy, each CR within the CCRs is modeled separately, resulting in a mathematical model that is the “sum” of multiple independent CR models [49], [52], [64]. When each CR can reach the desired target pose as intended, this approach enables efficient collaboration [108], [109]. However, when contact occurs between CRs or the modeling accuracy is insufficient, risks such as antagonism and collision may arise. To address these issues, a coupled modeling strategy can be adopted. This strategy builds upon independent modeling by incorporating geometric, velocity, and force constraints among the CRs to form a closed-loop kinematic chain, thereby constraining their relative motions. In this case, each CR’s workspace can be regarded as a chain space, while the overall workspace of the CCR constitutes the final task space, as shown in Fig. 3(a).

In both strategies, implementations are commonly based on the constant curvature (CC) assumption in geometric models and the Cosserat rod theory in physical models. The pseudo-rigid-body model [106], another geometric modeling approach, is less frequently employed.

1) *CC assumption*: As an idealized deformation paradigm for CRs, the CC assumption considers each segment of a deformed CR to be representable by a finite set of arc parameters [36], [80].

Let L denote the total length of the CR. For any point $s \in [0, L]$, the homogeneous transformation matrix $\mathbf{T}_t(\kappa, \phi, s) \in$

$\mathbb{R}^{4 \times 4}$ of a single segment is given by [107], [110]

$$\mathbf{T}_t(\kappa, \phi, s) = \begin{bmatrix} c\phi c\theta & -s\theta & c\phi s\theta & r c\phi(1 - c\theta) \\ s\phi c\theta & c\phi & s\phi s\theta & r s\phi(1 - c\theta) \\ -s\theta & 0 & c\theta & r s\theta \\ 0 & 0 & 0 & 1 \end{bmatrix}, \quad (1)$$

where κ is the curvature, $\theta = \kappa s$ is the bending angle, $r = 1/\kappa$ is the radius of curvature, and ϕ is the rotation angle about the base Z -axis. For notational simplicity, define $c\phi = \cos \phi$, $s\phi = \sin \phi$, $c\theta = \cos \theta$, and $s\theta = \sin \theta$.

Based on the CC assumption, the model can be further extended to piecewise constant curvature (PCC) by stacking multiple segments, enabling the modeling of multi-segment CRs. In PCC, the end-effector pose transformation matrix \mathbf{T}_{end} for a CR with n_{seg} segments can be obtained through chain multiplication [49], [64], [69]

$$\mathbf{T}_{\text{end}} = \prod_{i_{\text{seg}}=1}^{n_{\text{seg}}} \mathbf{T}_{i_{\text{seg}}}, \quad (2)$$

A schematic of the PCC model is shown in Fig. 3(b). By adopting idealized assumptions, this approach significantly improves the computational efficiency of the modeling process. However, because geometric models neglect the constitutive properties of the robot body and applied internal and external loads, these models may not fully capture CR behavior under physical contact, either between CRs or with the environment.

2) *Cosserat rod theory*: In the base coordinate frame, the position and orientation of an arbitrary point $s \in [0, L]$ along the CR can be described by a position vector field $\mathbf{P}(s) \in \mathbb{R}^3$ and an orientation matrix field $\mathbf{R}(s) \in \text{SO}(3)$. Additionally, the robot is subjected to an internal force $\mathbf{F}_{\text{in}}(s) \in \mathbb{R}^3$, an internal moment $\mathbf{L}_{\text{in}}(s) \in \mathbb{R}^3$, a distributed external force $\mathbf{F}(s) \in \mathbb{R}^3$, and an external moment $\mathbf{L}(s) \in \mathbb{R}^3$.

Based on this parameterization, the balance equations at s are established under the Newton–Euler framework as follows

[25], [67], [111], [112]

$$\begin{aligned}\frac{\partial \mathbf{P}(s)}{\partial s} &= \mathbf{K}_{\text{lin}}(s), \quad \frac{\partial \mathbf{R}(s)}{\partial s} = \hat{\mathbf{K}}_{\text{cur}}(s) \mathbf{R}(s), \\ \frac{\partial \mathbf{F}_{\text{in}}(s)}{\partial s} &= -\mathbf{F}(s), \\ \frac{\partial \mathbf{L}_{\text{in}}(s)}{\partial s} &= -\mathbf{L}(s) - \mathbf{K}_{\text{lin}}(s) \times \mathbf{F}_{\text{in}}(s),\end{aligned}\quad (3)$$

where $\mathbf{K}_{\text{cur}} \in \mathbb{R}^3$ and $\mathbf{K}_{\text{lin}}(s) \in \mathbb{R}^3$ represent the curvature and linear strain of the CR, respectively, and $\hat{\mathbf{K}}_{\text{cur}}(s)$ denotes the skew-symmetric matrix of $\mathbf{K}_{\text{cur}}(s)$ [30].

The above formulation yields a set of partial differential equations (PDEs) that describe the state of the CR. By incorporating appropriate boundary conditions and constraint equations, these PDEs can be solved using global approximation methods, such as the Ritz method [113], or local approximation methods, such as the shooting method [25], [112], [114]. To reduce computational complexity, the model can also be constructed under the Lagrangian framework based on the principle of minimum potential energy [115]. These 2 frameworks can be transformed into each other via Hamilton's principle (Fig. 3(c)) [116].

Fig. 3(c) illustrates the modeling schematic based on the Cosserat rod theory. By accounting for multiple deformation modes, modeling accuracy is significantly improved. However, the increased number of parameters involved leads to reduced computational efficiency.

In the modeling of CCRs, since they are often applied in relatively slow-operating scenarios such as surgical settings, inertial terms in their dynamics can usually be neglected. Conversely, at higher operating speeds, dynamic models should be considered. Table III provides a detailed comparison of the modeling methods reported in different references.

B. Formulation of coupling constraints

To achieve motion coordination among CRs, coupled modeling is more commonly employed. In the following, constraint construction methods are detailed according to different collaboration modes. Notably, mechanical constraints cannot be incorporated within the geometric models.

1) *Separate collaboration*: In the separate collaboration mode, the CR ends are typically assumed to be connected via a virtual rigid rod, as shown in Fig. 3(d). To ensure the validity of this connection, pose constraints must be satisfied at the connection points (1, c) and (2, c) between CR-1/CR-2 and the virtual rigid rod [68], [88], [117]

$$\begin{aligned}{}^M \mathbf{P}_{(1,c)} - {}^M \mathbf{P}_{(2,c)} - {}^M \mathbf{R}_{(2,c)} ({}^{2,c} \mathbf{P}_{(1,c)}) &= \mathbf{0}, \\ {}^M \mathbf{R}_{(1,c)} - {}^M \mathbf{R}_{(2,c)} ({}^{2,c} \mathbf{R}_{(1,c)}) &= \mathbf{0},\end{aligned}\quad (4)$$

where $\{M\}$ denotes the global frame, ${}^A \mathbf{P}_B \in \mathbb{R}^3$ is the position vector of point B expressed in frame $\{A\}$, and ${}^A \mathbf{R}_B \in \text{SO}(3)$ is the rotation matrix of the local frame at point B with respect to $\{A\}$.

These constraints can be extended to scenarios involving more CRs [118], enabling the formulation of a relative Jacobian matrix that directly constrains the inter-end-effector distances [57]. By specifying the length l_r and rotation angle

γ of the virtual rigid rod in ${}^A \mathbf{P}_B(l_r)$ and ${}^A \mathbf{R}_B(\gamma)$, respectively, Eq. (4) enables CR-2 to follow CR-1 in real time [119]. Furthermore, when manipulating deformable objects, the object can be modeled as a virtual flexible rod. Under the kinetostatics framework, force and moment constraints among the CRs can be formulated based on (4) [118].

2) *Assistance collaboration*: As shown in Fig. 3(e), in the assistance collaboration mode, the distal end of the support arm CR-2 is rigidly attached to the lateral side of the master arm CR-1. The pose constraints at the connection point must still satisfy Eq.(4). However, in this case, $({}^{2,c} \mathbf{R}_{(1,c)})$ is the identity matrix and $({}^{2,c} \mathbf{P}_{(1,c)})$ is the zero vector [111]. Based on this, additional constraints can be imposed to enforce equal linear and angular velocities at the connection point [30], [112]

$${}^M \mathbf{v}_{(1,c)} = {}^M \mathbf{v}_{(2,c)}, \quad {}^M \boldsymbol{\omega}_{(1,c)} = {}^M \boldsymbol{\omega}_{(2,c)}, \quad (5)$$

which enhance the system's responsiveness in dynamic environments. For multi-point connections with rotational DOFs, geometric constraints can be formulated based on the intersection and orthogonality of the two CRs' axes at the connection point, along with torque balance constraints [19]

$${}^M \mathbf{L}_{(1,c)} = {}^M \mathbf{L}_{(2,c)} = \mathbf{0}, \quad (6)$$

To improve computational efficiency, hybrid modeling is an effective solution. For instance, in cooperative sections subjected to interaction forces, Cosserat rod theory can be applied to model force constraints at the connection point. In contrast, for bending-only sections not subjected to interaction forces, the CC model can be adopted [99].

3) *Parallel collaboration*: In the parallel collaboration mode, the n CRs in the CCR are jointly connected to a mobile platform, and the backbone of each can be modeled as either a flexible rod or a combination of flexible and passive rigid rods [34], [106]. As the number of connection points increases, the system equilibrium shifts from the connection points to the center of the mobile platform, as illustrated in Fig. 3(f).

Based on the equilibrium point at the platform center, a closed-loop kinematic chain can be established for each CR, resulting in i position constraints (note that due to the use of spherical joint couplings, orientation constraints at the connection points are not required) [21], [106], [107]

$$\begin{aligned}{}^M \mathbf{P}_H + {}^M \mathbf{R}_H \cdot {}^H \mathbf{P}_{(i,c)} - {}^M \mathbf{P}_i - {}^M \mathbf{R}_H \cdot l_c \cdot \mathbf{e}_3 &= \mathbf{0}, \\ i &= 1, 2, \dots, n,\end{aligned}\quad (7)$$

where $\{H\}$ denotes the frame at the center of the mobile platform, ${}^H \mathbf{P}_{(i,c)} \in \mathbb{R}^3$ is the offset vector of the i -th connection point in frame $\{H\}$, ${}^M \mathbf{P}_i \in \mathbb{R}^3$ is the end position of the i -th CR in the global frame $\{M\}$, l_c is the length of the passive rigid rod, and $\mathbf{e}_3 = [0, 0, 1]^T$ represents the unit vector along the local z-axis of the CR.

Furthermore, force and torque balance constraints can be imposed at the mobile platform center [113]

$$\begin{aligned}{}^M \mathbf{F}_e - \sum_{i=1}^n \left({}^M \mathbf{F}_{\text{in},i} - \sum_k {}^M \mathbf{F}_{(k,i)} \right) &= \mathbf{0}, \\ {}^M \mathbf{L}_e - \sum_{i=1}^n \left(\mathbf{r}_i \times \left({}^M \mathbf{F}_{\text{in},i} - \sum_k {}^M \mathbf{F}_{(k,i)} \right) \right) &= \mathbf{0},\end{aligned}\quad (8)$$

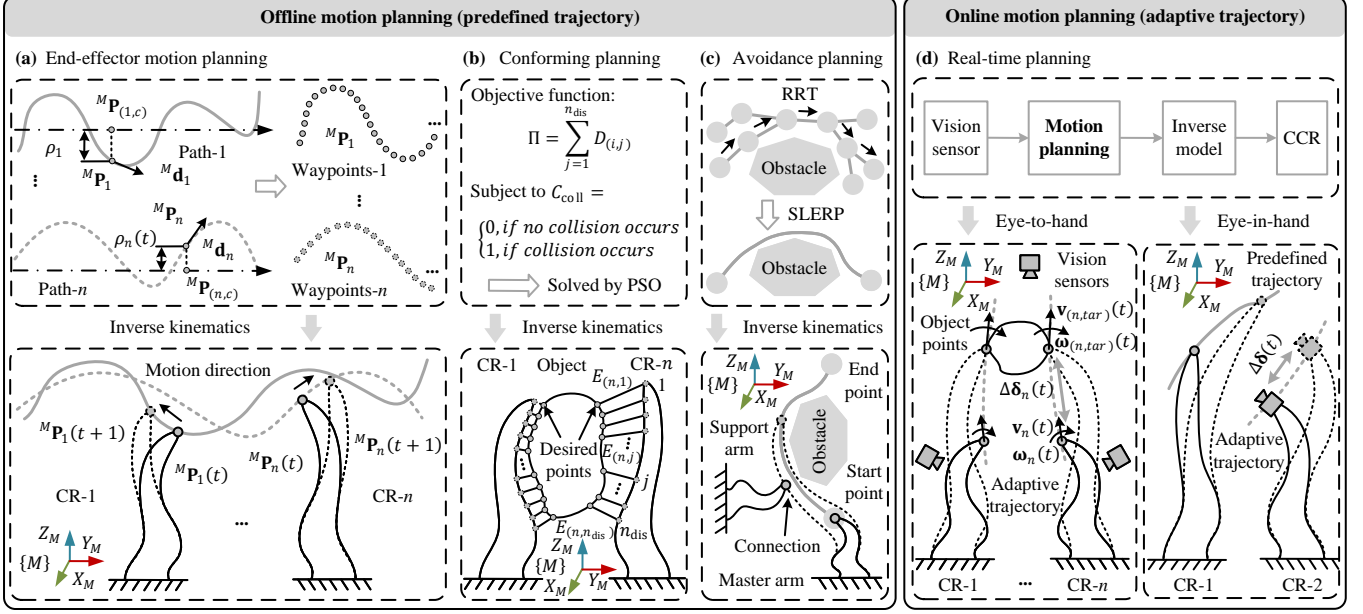


Fig. 4. Motion planning methods for CCRs. (a) End-effector planning. (b) Conforming planning. (c) Avoidance planning. (d) Real-time planning.

where ${}^M\mathbf{F} \in \mathbb{R}^3$ and ${}^M\mathbf{L} \in \mathbb{R}^3$ denote the external force and moment acting at the platform center. ${}^M\mathbf{F}_{\text{in},i}$ is the internal force at the end of the i -th CR, and ${}^M\mathbf{F}_{(k,i)}$ represents the tensile force of the k -th tendon in the i -th CR, typically with $k \in \{1, 2, 3, 4\}$. The moment arm vector is given by $\mathbf{r}_i = {}^M\mathbf{R}_H \cdot {}^H\mathbf{P}_{(i,c)} \in \mathbb{R}^3$.

C. Summary

Across the three collaboration modes, the modeling of CCRs typically relies on geometric and physical models and is evolving from independent to coupled modeling, thereby reducing antagonistic interactions and collision risks among multiple CRs. However, under complex loads and constraints, geometric models often fail to capture the nonlinear deformation and mechanical constraints of individual CRs, whereas physical models are computationally intensive, making it difficult for existing modeling approaches to balance efficiency and accuracy [120]. This issue becomes particularly pronounced in assistance and parallel collaboration, where mechanical linkages further increase coupling complexity.

IV. MOTION PLANNING AND CONTROL OF CCRs

The collaboration of multiple CRs within a CCR increases the complexity of its motion. To ensure precise execution of target tasks while avoiding collision risks, motion planning and control should be performed at higher temporal and spatial levels of the system architecture. In this section, the motion planning approaches and control strategies for CCRs are presented and analyzed.

A. Motion planning of CCRs

Defining an appropriate motion path serves as a guideline for accomplishing the target task. In current research, motion planning methods can be broadly classified into online and offline approaches.

1) *Offline Motion Planning*: This approach refers to pre-planning the motion paths of each CR within the CCR workspace according to the task requirements before the target task begins, without further updates during execution. In this approach, the motion path ${}^M\mathbf{P}_i = [x_i, y_i, z_i]^T$ can be defined by specifying the functional forms of a baseline and a pose offset (Fig. 4(a)) [7]

$${}^M\mathbf{P}_i = {}^M\mathbf{P}_{(i,c)} + \rho_i {}^M\mathbf{d}_i, \quad (9)$$

where ${}^M\mathbf{P}_{(i,c)} = [x_{(i,c)}, y_{(i,c)}, z_{(i,c)}]^T$ denotes the position of the reference center point of the i -th path corresponding to the CR- i , ρ_i is the offset radius of the path, and ${}^M\mathbf{d}_i \in \mathbb{R}^3$ is the direction vector of the path. As a simplified approach, it is more common in the three collaboration modes of CCRs to directly specify discrete waypoints ${}^M\mathbf{P}_i$ of the CR- i end-effectors contained in the CCR [29], [57], [121], [122]. Based on this, adding time constraints t enables the realization of offline trajectory planning [72].

In separated collaboration, CCR grasping mechanisms have been investigated, with [117] proposing taxonomies and quantitative metrics for grasp quality, and [123] further identifying optimal grasp configurations and contact points, thereby enhancing grasp performance. To further plan the sections of the CCR other than the end-effector, the optimization objective Π can be defined to minimize the distances $D_{(i,j)} (j \in \{1, 2, \dots, n_{\text{dis}}\})$ between discrete points j on the CR- i and the corresponding discrete points on the target surface, while ensuring collision-free operation with the environment through a collision constraint C_{coll} . This problem can be solved using the adaptive particle swarm optimization (PSO) algorithm, enabling complete conforming planning (Fig. 4(b)) [75]. In more complex environments, it is necessary to address constraint C_{coll} to achieve avoidance planning and ensure operational safety. One approach is to analyze the workspace of each CR to identify regions with potential collision risks and remove these

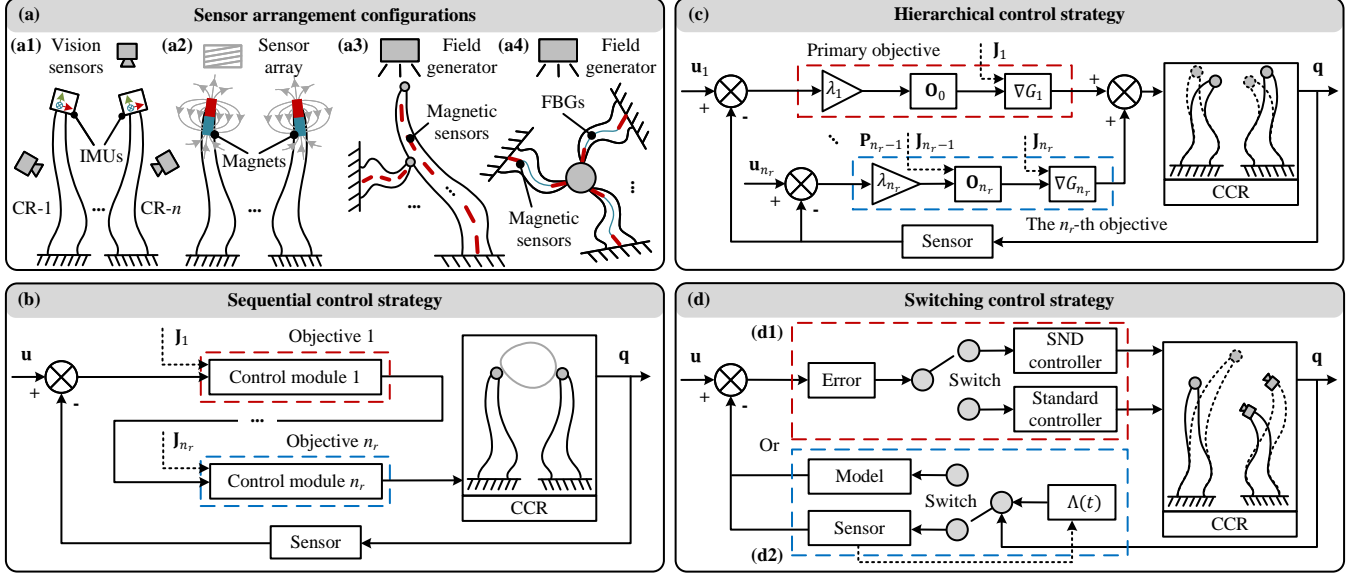


Fig. 5. Control of CCRs. (a) Sensor arrangement configurations. (b) Sequential control strategy. (c) Hierarchical control strategy. (d) Switching control strategy.

regions from the actuation space, based on inverse kinematics results, to prevent collisions [124]. To further avoid collisions involving sections of a CR other than the end-effector, each CR can be discretized into n_{dis} segments, and the Euclidean distance from a segment on one CR to potentially colliding segments on other CRs can be computed, with the minimum distance constrained to exceed a predefined threshold [125].

In assistance collaboration, the configuration space of the CCR can be sampled on an occupancy grid map using the rapidly-exploring random trees (RRT) method. During the tree expansion process, collision checking is continuously performed based on forward kinematics, and spherical linear interpolation (SLERP) is applied to maintain interpolation continuity, thereby generating a feasible trajectory for the master arm end-effector (Fig. 4(c)) [126].

2) *Online Motion Planning*: To enhance the adaptability of CCRs in dynamic environments, online motion planning can be adopted. To date, this approach has only been demonstrated in the separated collaboration mode, where real-time visual feedback is used to update CR motion states within each control cycle. Depending on the placement of vision sensors, two configurations can be distinguished: eye-to-hand [107], [108] and eye-in-hand [119], [127], [128], as shown in Fig. 4(d).

In the eye-to-hand configuration, multiple external vision sensors continuously compute the pose deviation of each CR end-effector relative to its corresponding desired point: $\Delta\delta_i(t) = [\Delta\mathbf{P}_i(t), \Delta\mathbf{R}_i(t)]^T$. Based on this deviation, the desired velocity is planned as [68]

$$\hat{\delta}_i(t) = f_{\delta}(\Delta\delta_i(t), \hat{\delta}_{(i,\text{tar})}(t)), \quad (10)$$

where $\hat{\delta}_{(i,\text{tar})}(t) = [\mathbf{v}_{(i,\text{tar})}(t), \boldsymbol{\omega}_{(i,\text{tar})}(t)]^T$ denotes the linear and angular velocities of the desired point. Although this sensing configuration also appears in the other two collaboration modes [21], [30], no dedicated methods have been reported for them.

In the eye-in-hand configuration, the observed CR moves along a predefined offline trajectory or under manual operation, while the CR carrying the vision sensors computes the pose deviation $\Delta\delta_i(t)$ between its current pose and the target point on the observed CR in real time. Visual servoing is then used to achieve tracking [99]. Although existing studies on the eye-in-hand configuration have not examined the motion planning process in detail, the implementation principle is similar to that of the eye-to-hand configuration and can, in theory, enable online updates of the end-effector velocity.

B. Control of CCRs

Once the target path/trajectory has been obtained, establishing an appropriate control strategy is essential to ensure precise task execution. Currently, most CCRs still employ open-loop control, as optimization in structural design can partially improve motion accuracy [29]. A commonly used approach is the open-loop master-slave control strategy, in which a master device captures the operator's force signals and transmits them as motion commands to the slave CCR for remote execution of the corresponding actions [17], [50], [51], [58], [129]. However, because this approach relies on feedback derived from the operator's perception, its performance is highly dependent on the operator's experience. Moreover, in complex task environments, open-loop control can introduce greater uncertainty [29].

1) *Feedback mechanisms*: The key challenge in closed-loop control is accurately estimating and feeding back each CR's pose in real time to enable error computation and actuation updates [130].

Visual-based feedback is the most widely used approach across the three collaborative modes, with sensor placement typically following two configurations (Fig. 4(c)). Pose estimation can be achieved either by detecting fiducial markers mounted on the CR surface [68], [107], [131]–[136] or by applying deep learning algorithms to markerless CR images

TABLE IV
COMPARISON OF CONTROL STRATEGIES FOR CCRs

Ref.	Mode	Feedback mech.	Open/Closed Loop	Control strategy	Position error	Orientation error	Force error
[50]	SC	VS	Open	Master-slave	—	—	—
[58]	SC	VS-FS-ES	Open	Master-slave	—	—	—
[51]	SC	VS-ES	Open	Master-slave	RE(LE): 0.500 mm~2.800 mm (0.890%~5.000%)	1.800°	—
[128]	SC	VS-FS	Open	Master-slave	—	—	1.020 N
[17]	SC	VS	Open	Master-slave	1.340 mm (1.340%)	—	—
[118]	SC	VS	Closed	Sequential	1.040 mm~2.510 mm 0.200 mm~0.899 mm (0.111%~0.499%)	1.350°~3.960°	—
[68]	SC	Simulation	Closed	Sequential	0.005°~0.523°	0.025 N~0.340 N	—
[121]	SC	ES	Closed	Hierarchical	PE: 0.230 mm~0.380 mm (0.413%~0.682%)	0.005°	—
[57]	SC	ES	Closed	Hierarchical	PE: 0.650 mm (1.300%)	—	—
[125]	SC	Simulation	Closed	Hierarchical	PE: 0.396 mm (0.863%)	—	—
[99]	SC	VS	Closed	Switching	—	—	—
[131]	SC	VS	Closed	Switching	0.650 mm	1.050°	—

SC: Separated Collaboration

VS: Vision Sensor; FS: Force Sensor; ES: Electromagnetic Tracking Sensor

RE: Repeatability Error; PE: Primary Objective Error; LE: Load Error

[137]. When combined with geometric parameter identification, these methods can further enhance measurement accuracy [21]. However, a major challenge remains the synchronized perception of multiple CRs, as the accuracy of visual sensing is highly sensitive to inter-CR occlusions, environmental obstacles, and poor lighting conditions [38].

To address these challenges, two representative strategies have been proposed. First, visual sensors can be combined with inertial measurement units (IMUs) mounted on each CR to estimate the end-effector pose (Fig. 5(a1)), thereby improving robustness against external disturbances [138]. Second, embedded sensors can be integrated with state estimation methods to achieve CCR pose perception. In the separated cooperation mode, [131] embedded permanent magnets at each CR end-effector and employed an external magnetic sensor array (Fig. 5(a2)). By fusing a PCC prior with a multi-dipole magnetic model in an extended Kalman filter, thereby enabling real-time tracking of multiple CR end-effectors. In the assistance mode, [114] placed magnetic sensors discretely along the backbone (Fig. 5(a3)). By combining a Cosserat-rod prior with forward extended Kalman–Bucy filtering over arc length and Rauch–Tung–Striebel smoothing, thereby enabling shape estimation under unknown end-effector loads. Furthermore, [139] combined magnetic sensors at the base and end-effector with fiber Bragg grating (FBG) strain sensors along the backbone (Fig. 5(a4)). By introducing a constant-strain Gaussian process prior on $SE(3)$ and performing maximum a posteriori estimation within a sparse factor-graph framework, coupling constraints were encoded as factors, thereby enhancing the real-time performance and robustness of sensing. The method can also be extended to parallel cooperation. Notably, further efforts are needed to integrate these feedback strategies with control frameworks to fully demonstrate the advantages of feedback mechanisms.

2) *Control Strategies*: To further enhance the performance of CCRs, control strategies should be designed based on feedback mechanisms [72]. At present, most strategies focus on the separated collaborative mode and are typically model-

based. Unlike single CRs, CCRs require synchronous control of multiple end-effectors to ensure coordinated task execution, which is usually achieved by combining the Jacobian matrices of the n CRs into a unified Jacobian \mathbf{J} [57], [108], [109], [121], [125]. On this basis, existing strategies can be broadly categorized into three classes, namely sequential, hierarchical and switching (Table IV).

The control of CCRs often involves multiple objectives, which may occur within the same or across different control cycles. For objectives within the same cycle, a straightforward approach is to adopt a sequential control strategy (Fig. 5(b)), where different objectives are handled in order. For example, [118] first minimizes the residual of end-effector pose and force–balance constraints before incorporating deformation energy minimization, whereas [68] first enforces end-effector pose and closure constraints before minimizing equivalent joint torques. To further prevent conflicts among tasks, a hierarchical control strategy can be constructed by assigning importance levels to each objective (Fig. 5(c)) [121]

$$\mathbf{q} = \sum_{r=1}^{n_r} \lambda_r \mathbf{O}_{r-1} \nabla G_r, \quad (11)$$

where \mathbf{q} denotes the system output, $\lambda_r (r = 1, 2, \dots, n_r)$ is the weighting coefficient of task r , ∇G_r represents the control gradient of objective r , and \mathbf{O}_{r-1} is the null-space projection matrix of the first $(r-1)$ objectives. The projection matrix can be recursively constructed as

$$\mathbf{O}_r = \mathbf{O}_{r-1} - (\mathbf{J}_r \mathbf{O}_{r-1})^\dagger (\mathbf{J}_r \mathbf{O}_{r-1}), \quad \mathbf{O}_0 = \mathbf{I}, \quad (12)$$

where $(\cdot)^\dagger$ denotes the Moore–Penrose pseudoinverse. By sequentially projecting each task into the null-space of higher-hierarchical objectives, this scheme enables the decoupling and coordination of multiple objectives, including end-effector relative position maintenance, inter-CR collision avoidance, trajectory tracking, and manipulability optimization [57], [125].

In addition, objectives across different control cycles can be coordinated by introducing a threshold parameter to switch between control modes. For instance, [99] specifies that when

the pose error exceeds threshold parameter, a normalized controller based on the normalized Jacobian \mathbf{J}_{std} is employed to ensure faster convergence; otherwise, the system switches to a standard controller based on the standard Jacobian \mathbf{J}_{S} to achieve higher accuracy (Fig. 5(d1)). Similarly, [133] defines a perception state parameter $\Lambda(t)$, where $\Lambda(t) = 1$ activates the closed-loop mode and $\Lambda(t) = 0$ switches to the open-loop mode, thereby enhancing system robustness (Fig. 5(d2)).

From another perspective, CCRs can be regarded as a type of multi-robot system [140]. Most existing studies employ centralized control, as this approach ensures effective coordination among individual CRs. However, with an increasing number of CRs, centralized architectures impose substantial computational burdens. In this context, decentralized control [141] offers a promising alternative to mitigate these challenges.

C. Summary

At higher system architecture levels, motion planning approaches and control strategies remain at an early stage of development. Existing control strategies are largely concentrated in the separated collaboration mode, whereas studies on the assistance and parallel modes remain focused on feedback mechanisms, and the control strategies in these two modes are still limited. In the separated mode, a common practice is to perform offline motion planning by jointly considering inter-CR cooperation and collision-avoidance constraints, and then execute tasks with model-based control. Although offline planning and model-based control can provide effective guidance, in dynamic environments offline trajectories are difficult to update promptly, and limited observability caused by constrained sensor placement further degrades performance, both of which may lead to task failure.

V. CHALLENGES AND OPPORTUNITIES

Despite substantial progress in CCRs over the past decade, many challenges remain unresolved. In this section, current challenges and future opportunities for CCRs are outlined, followed by a discussion of potential application.

A. Intelligent structural design

For task-specific objectives, the structural design of CCRs requires balanced trade-offs to achieve optimal configurations [19]. However, existing studies primarily enhance a single performance dimension through simplified task analyses or bioinspired heuristics, followed by parameter tuning in multi-objective optimization. Such approaches remain highly dependent on the designer's expertise and hinder the realization of optimal design trade-offs in CCRs.

To address these challenges, future research can refer to and combine relevant advances in artificial intelligence and design theory to expand existing CCR design methods. Deep-level requirement mining in design theory [142] should be considered first as the foundation of structural design. At the same time, by building a knowledge graph to systematically summarize and reuse design experience reported in CCR publications and patents [143], [144], a large language model for CCRs can be constructed to guide detailed design.

B. Physics-informed data-driven modeling

Establishing mathematical models that map the actuation space to the workspace is another research priority in the CCRs field. To balance efficiency and accuracy in the modeling process, data-driven approaches have been introduced [108], [109]. However, these methods generally suffer from limited interpretability and insufficient generalization [120].

To address these challenges, physics-informed neural networks (PINNs) are promising for broad application in this field. By embedding physical constraints in the loss function, PINNs can improve physical consistency and reduce reliance on large experimental datasets [145]. Although initial validation has been demonstrated for single-CR modeling [146], coupled modeling strategies for CCRs still require in-depth investigation. In particular, for flexible-object grasping in the separated collaboration mode, it is necessary to extend the geometric constraints between the CCR and the flexible object to constitutive relations for deformable objects [118], so as to more accurately describe interactions between the CCR and the environment and thereby enhance grasping performance.

C. Reinforcement learning-based planning and control

Current motion planning and control methods for CCRs still face multiple challenges, including limited real-time adaptability to dynamic environments and insufficient observability caused by constraints on sensor deployment.

To address these challenges, reinforcement learning (RL) based motion planning and control [147], [148] offer a new direction for CCRs. This approach has already been adopted in certain dexterous hands and merits broader application in CCRs [149]–[151]. By interacting with the environment, RL can autonomously learn adaptive policies that balance cooperation and obstacle avoidance without relying on precise models or heavy preprocessing, while supporting continual updating and generalization [130]. This indicates promise across all three collaboration modes. At the algorithmic level, imitation learning [152] can reduce sample complexity, and game-theoretic methods [153] can strengthen multi-CR cooperation under uncertainty, together enabling real-time planning and robust control. At the hardware level, constructing CCR bodies with self-sensing smart materials [154], [155] can avoid sensor-placement occlusion and accuracy issues, thereby providing stronger support for RL deployment.

D. Potential applications

To date, CCRs have been widely applied in surgical and industrial domains, including natural-orifice transluminal endoscopic surgery, single-port access surgery, aero-engine maintenance, on-orbit capture, and object grasping, with favorable outcomes. However, most CCRs remain at the research or prototype stage rather than being deployed in practice, leaving many potential application scenarios underexplored and the intrinsic advantages of CCRs underutilized. Accordingly, based on an analysis of CCR advantages, several representative opportunities are outlined below.

1) *Rehabilitation*: Experiments have shown that interactions such as hugging with rigid collaborative robots sheathed in soft materials [156] can effectively reduce patient stress [157]. Introducing CCRs with higher compliance could further broaden the range of safe interactions between humans and robots and thereby improve the effectiveness of rehabilitation training, showing considerable promise.

2) *Emergency response*: Disaster-relief environments are often narrow with tortuous paths, and conventional articulated robots, constrained by rigid links and limited joint ranges, struggle to access target areas [158], [159]. Leveraging the compliance and collaborative capabilities of CCRs could enable environmental probing, payload delivery, in-cavity disassembly, and rescue operations in such extreme settings, thereby increasing the likelihood of successful rescue.

3) *Agriculture*: In fruit and vegetable harvesting, the high compliance of CCRs allows them to reach into gaps between leaves and branches [160], [161], while maintaining conformity to delicate plants. With onboard shape and force sensing, real-time perception and feedback control could be implemented, with the potential to reduce damage risk to crops and thereby improve harvesting efficiency.

VI. CONCLUSION

CCRs offer unique advantages over single CRs, including enhanced task adaptability, expanded workspace, improved flexibility, increased load capacity, and greater operational stability, thereby enabling a wider range of applications. By defining three modes of CCR collaboration, reviewing research progress in structural design, modeling, motion planning, and control, and discussing current challenges and future opportunities, this survey provides CCR researchers with a clear overview of the field from different system-architecture levels.

In future research, emphasis should be placed on intelligent structural design, physics-informed data-driven modeling, and RL-based planning and control. These directions are expected to significantly enhance CCR performance and broaden their application in areas such as rehabilitation, emergency response, and agriculture.

REFERENCES

- [1] C. Laschi and B. Mazzolai, “Lessons from animals and plants: The symbiosis of morphological computation and soft robotics,” *IEEE Robot. Autom. Mag.*, vol. 23, no. 3, pp. 107–114, 2016.
- [2] M. Li, A. Pal, A. Aghakhani, A. Pena-Francesch, and M. Sitti, “Soft actuators for real-world applications,” *Nat. Rev. Mater.*, vol. 7, no. 3, pp. 235–249, 2022.
- [3] X. Dong, D. Palmer, D. Axinte, and J. Kell, “In-situ repair/maintenance with a continuum robotic machine tool in confined space,” *J. Manuf. Process.*, vol. 38, pp. 313–318, 2019.
- [4] Y. Kong *et al.*, “Concentric wire-driven robots with in situ torsion for transnasal surgery,” *IEEE/ASME Trans. Mechatron.*, vol. 30, no. 1, pp. 599–610, 2024.
- [5] L. Raimondi, M. Russo, X. Dong, A. Norton, and D. Axinte, “A miniaturized tendon-driven continuum robot for direct laser deposition,” *IEEE Robot. Autom. Lett.*, vol. 10, no. 10, pp. 9686–9693, 2025.
- [6] J. Liu *et al.*, “An underwater robotic system with a soft continuum manipulator for autonomous aquatic grasping,” *IEEE/ASME Trans. Mechatron.*, vol. 29, no. 2, pp. 1007–1018, 2023.
- [7] E. Quaicoe, A. Nada, H. Ishii, and H. El-Hussieny, “Cooperative control of bimanual continuum robots for automated knot-tying in robot-assisted surgical suturing,” *J. Robot. Control*, vol. 5, no. 4, pp. 1149–1165, 2024.
- [8] D. Fonseca and P. Neto, “Electrically-driven phase transition actuators to power soft robot designs,” *Nat. Commun.*, vol. 16, no. 1, 2025, Art. no. 3820.
- [9] L. Zhao, Y. Jiang, C.-Y. She, M. Chen, and D. Balkcom, “Softsnap: Rapid prototyping of untethered soft robots using snap-together modules,” *Soft Robot.*, early access, Jun. 2025.
- [10] D. Grace *et al.*, “Development of a novel six dof soft parallel robot,” in *Proc. SoutheastCon 2022*. IEEE, 2022, pp. 81–86.
- [11] Q. Wu, H. Zhao, X. Chen, and Y. Zhao, “Review of technology, application status and development trend in multi-arm cooperative robots,” *J. Mech. Eng.*, vol. 59, no. 15, pp. 1–16, 2023.
- [12] J. Salisbury and G. Guthart, “The intuitive™ telesurgery system: Overview and application,” in *Proc. 2000 IEEE Int. Conf. Robot. Automat. (ICRA)*. IEEE, 2000, pp. 618–621.
- [13] M. P. Polverini, A. M. Zanchettin, and P. Rocco, “A constraint-based programming approach for robotic assembly skills implementation,” *Robot. Comput. Manuf.*, vol. 59, pp. 69–81, 2019.
- [14] K. L. Yung, J. Cheung, S. Chung, S. Singh, and C. Yeung, “A single-port robotic platform for laparoscopic surgery with a large central channel for additional instrument,” *Ann. Biomed. Eng.*, vol. 45, no. 9, pp. 2211–2221, 2017.
- [15] Y. Kobayashi *et al.*, “Development of a robotic system with six-degrees-of-freedom robotic tool manipulators for single-port surgery,” *Int. J. Med. Robot. Comput. Assist. Surg.*, vol. 11, no. 2, pp. 235–246, 2015.
- [16] X. Dong *et al.*, “Continuum robots collaborate for safe manipulation of high-temperature flame to enable repairs in challenging environments,” *IEEE/ASME Trans. Mechatron.*, vol. 27, no. 5, pp. 4217–4220, 2022.
- [17] Y. Chen *et al.*, “The shurui system: a modular continuum surgical robotic platform for multiport, hybrid-port, and single-port procedures,” *IEEE/ASME Trans. Mechatron.*, vol. 27, no. 5, pp. 3186–3197, 2021.
- [18] J. Burgner *et al.*, “A telerobotic system for transnasal surgery,” *IEEE/ASME Trans. Mechatron.*, vol. 19, no. 3, pp. 996–1006, 2013.
- [19] A. W. Mahoney, P. L. Anderson, P. J. Swaney, F. Maldonado, and R. J. Webster, “Reconfigurable parallel continuum robots for incisionless surgery,” in *Proc. 2016 IEEE/RSJ Int. Conf. Intell. Robots Syst. (IROS)*. IEEE, 2016, pp. 4330–4336.
- [20] M. C. Lastinger, S. Verma, A. D. Kapadia, and I. D. Walker, “Tree: A variable topology, branching continuum robot,” in *Proc. 2019 IEEE Int. Conf. Robot. Automat. (ICRA)*. IEEE, 2019, pp. 5365–5371.
- [21] Z. Wang *et al.*, “Development of a new cable-driven planar parallel continuum robot using compound kinematic calibration method,” *J. Mech. Robot.*, vol. 16, no. 10, 2024, Art. no. 101014.
- [22] R. J. Hendrick, C. R. Mitchell, S. D. Herrell, and R. J. Webster III, “Hand-held transendoscopic robotic manipulators: A transurethral laser prostate surgery case study,” *Int. J. Robot. Res.*, vol. 34, no. 13, pp. 1559–1572, 2015.
- [23] P. Yang, L. Mao, C. Tian, X. Meng, and H. Xie, “A cooperative and multifunctional magnetic continuum robot for noninteractive access, dexterous navigation, and versatile manipulation,” *Adv. Funct. Mater.*, vol. 35, no. 2, 2025, Art. no. 2412543.
- [24] Z. Mitros *et al.*, “Optic nerve sheath fenestration with a multi-arm continuum robot,” *IEEE Robot. Autom. Lett.*, vol. 5, no. 3, pp. 4874–4881, 2020.
- [25] J. Wang, J. Peine, and P. E. Dupont, “Eccentric tube robots as multiarmed steerable sheaths,” *IEEE Trans. Robot.*, vol. 38, no. 1, pp. 477–490, 2021.
- [26] Y. Li *et al.*, “A dual-mode actuator for soft robotic hand,” *IEEE Robot. Autom. Lett.*, vol. 6, no. 2, pp. 1144–1151, 2021.
- [27] K. Becker *et al.*, “Active entanglement enables stochastic, topological grasping,” *Proc. Natl. Acad. Sci.*, vol. 119, no. 42, 2022, Art. no. e2209819119.
- [28] Z. Wang, N. M. Freris, and X. Wei, “Spirobs: Logarithmic spiral-shaped robots for versatile grasping across scales,” *Device*, vol. 3, no. 4, 2025, Art. no. 100646.
- [29] Q. Ji *et al.*, “Omnidirectional walking of a quadruped robot enabled by compressible tendon-driven soft actuators,” in *Proc. 2022 IEEE/RSJ Int. Conf. Intell. Robots Syst. (IROS)*. IEEE, 2022, pp. 11015–11022.
- [30] A. Jalali and F. Janabi-Sharifi, “Dynamic manipulation and stiffness modulation of cooperative continuum robots: Theory and experiment,” *J. Mech. Robot.*, vol. 16, no. 12, 2024, Art. no. 121001.
- [31] M. Russo *et al.*, “Cooperative continuum robots: Enhancing individual continuum arms by reconfiguring into a parallel manipulator,” *IEEE Robot. Autom. Lett.*, vol. 7, no. 2, pp. 1558–1565, 2021.
- [32] Y. Cai *et al.*, “Modular self-reconfigurable continuum robot for general purpose loco-manipulation,” *IEEE Robot. Autom. Lett.*, vol. 10, no. 2, pp. 1976–1983, 2025.

[33] L. Mao *et al.*, "Magnetic steering continuum robot for transluminal procedures with programmable shape and functionalities," *Nat. Commun.*, vol. 15, no. 1, 2024, Art. no. 3759.

[34] S. Lilge, K. Nuelle, G. Boettcher, S. Spindeldreier, and J. Burgner-Kahrs, "Tendon actuated continuous structures in planar parallel robots: A kinematic analysis," *J. Mech. Robot.*, vol. 13, no. 1, 2021, Art. no. 011025.

[35] G. Böttcher, S. Lilge, and J. Burgner-Kahrs, "Design of a reconfigurable parallel continuum robot with tendon-actuated kinematic chains," *IEEE Robot. Autom. Lett.*, vol. 6, no. 2, pp. 1272–1279, 2021.

[36] Z. Yang, X. Zhu, and K. Xu, "Continuum delta robot: A novel translational parallel robot with continuum joints," in *Proc. 2018 IEEE/ASME Int. Conf. Adv. Intell. Mechatron. (AIM)*. IEEE, 2018, pp. 748–755.

[37] W. Zhang *et al.*, "Research progress and development trend of surgical robot and surgical instrument arm," *Int. J. Med. Robot. Comput. Assist. Surg.*, vol. 17, no. 5, 2021, Art. no. e2309.

[38] N. Simaan, R. M. Yasin, and L. Wang, "Medical technologies and challenges of robot-assisted minimally invasive intervention and diagnostics," *Annu. Rev. Control Robot. Auton. Syst.*, vol. 1, no. 1, pp. 465–490, 2018.

[39] Y. Cao *et al.*, "Continuum robots for endoscopic sinus surgery: Recent advances, challenges, and prospects," *Int. J. Med. Robot. Comput. Assist. Surg.*, vol. 19, no. 2, 2023, Art. no. e2471.

[40] G. Chen, S. Tang, X. Duan, and H. Wang, "Design, modeling, and evaluation of parallel continuum robots: A survey," *Sci. China Technol. Sci.*, vol. 67, no. 3, pp. 673–695, 2024.

[41] S. Lilge *et al.*, "Parallel-continuum robots: a survey," *IEEE Trans. Robot.*, vol. 40, pp. 3252–3270, 2024.

[42] J. Langowski, P. Sharma, and A. L. Shoultari, "In the soft grip of nature," *Sci. Robot.*, vol. 5, no. 49, 2020, Art. no. eabd9120.

[43] J. Hernandez *et al.*, "Current designs of robotic arm grippers: A comprehensive systematic review," *Robotics*, vol. 12, no. 1, 2023, Art. no. 5.

[44] M. Pozzi, M. Malvezzi, D. Pratichizzo, and G. Salvietti, "Actuated palms for soft robotic hands: review and perspectives," *IEEE/ASME Trans. Mechatron.*, vol. 29, no. 2, pp. 902–912, 2023.

[45] Y. Shan *et al.*, "Variable stiffness soft robotic gripper: design, development, and prospects," *Bioinspir. Biomim.*, vol. 19, no. 1, 2023, Art. no. 011001.

[46] J. Zhang *et al.*, "Dexterous hand towards intelligent manufacturing: A review of technologies, trends, and potential applications," *Robot. Comput. Manuf.*, vol. 95, 2025, Art. no. 103021.

[47] Z. Yu, A. Duan, Z. Zhu, and W. Zhang, "Biomimetic soft-legged robotic locomotion, interactions and transitions in terrestrial, aquatic and multiple environments," *Sustain. Mater. Technol.*, vol. 40, 2024, Art. no. e00930.

[48] H. Yu, L. Wu, K. Wu, and H. Ren, "Development of a multi-channel concentric tube robotic system with active vision for transnasal nasopharyngeal carcinoma procedures," *IEEE Robot. Autom. Lett.*, vol. 1, no. 2, pp. 1172–1178, 2016.

[49] N. Ma, S. Monk, and D. Cheneler, "Collaborative continuum robots for remote engineering operations," *Biomimetics*, vol. 8, no. 1, 2022, Art. no. 4.

[50] A. De Donno, L. Zorn, P. Zanne, F. Nageotte, and M. de Mathelin, "Introducing stras: A new flexible robotic system for minimally invasive surgery," in *Proc. 2013 IEEE Int. Conf. Robot. Automat. (ICRA)*. IEEE, 2013, pp. 1213–1220.

[51] M. Hwang and D.-S. Kwon, "Strong continuum manipulator for flexible endoscopic surgery," *IEEE/ASME Trans. Mechatron.*, vol. 24, no. 5, pp. 2193–2203, 2019.

[52] T. Cheng, G. Zhang, J. Sun, T. Zhang, and F. Du, "Dexterity enhancement of continuum robot for natural orifice transluminal endoscopic surgery in the dual-manipulator collaborative space," *Int. J. Med. Robot. Comput. Assist. Surg.*, vol. 19, no. 4, 2023, Art. no. e2516.

[53] E. Amanov *et al.*, "Transurethral anastomosis after transurethral radical prostatectomy: a phantom study on intraluminal suturing with concentric tube robots," *IEEE Trans. Med. Robot. Bionics*, vol. 2, no. 4, pp. 578–581, 2020.

[54] R. J. Hendrick, S. D. Herrell, and R. J. Webster, "A multi-arm handheld robotic system for transurethral laser prostate surgery," in *Proc. 2014 IEEE Int. Conf. Robot. Automat. (ICRA)*. IEEE, 2014, pp. 2850–2855.

[55] K. Price *et al.*, "Using robotics to move a neurosurgeon's hands to the tip of their endoscope," *Sci. Robot.*, vol. 8, no. 82, 2023, Art. no. eadg6042.

[56] R. E. Goldman *et al.*, "Design and performance evaluation of a minimally invasive telerobotic platform for transurethral surveillance and intervention," *IEEE Trans. Biomed. Eng.*, vol. 60, no. 4, pp. 918–925, 2012.

[57] M. T. Chikhaoui, J. Granna, J. Starke, and J. Burgner-Kahrs, "Toward motion coordination control and design optimization for dual-arm concentric tube continuum robots," *IEEE Robot. Autom. Lett.*, vol. 3, no. 3, pp. 1793–1800, 2018.

[58] M. Hwang and D.-S. Kwon, "K-flex: a flexible robotic platform for scar-free endoscopic surgery," *Int. J. Med. Robot. Comput. Assist. Surg.*, vol. 16, no. 2, 2020, Art. no. e2078.

[59] Y. Lei, Y. Li, R. Song, and F. Du, "Development of a novel deployable arm for natural orifice transluminal endoscopic surgery," *Int. J. Med. Robot. Comput. Assist. Surg.*, vol. 17, no. 3, 2021, Art. no. e2232.

[60] E. Amanov, T.-D. Nguyen, S. Markmann, F. Imkamp, and J. Burgner-Kahrs, "Toward a flexible variable stiffness endoport for single-site partial nephrectomy," *Ann. Biomed. Eng.*, vol. 46, no. 10, pp. 1498–1510, 2018.

[61] C. Li, X. Gu, X. Xiao, C. M. Lim, and H. Ren, "A robotic system with multichannel flexible parallel manipulators for single port access surgery," *IEEE Trans. Ind. Inf.*, vol. 15, no. 3, pp. 1678–1687, 2018.

[62] B. L. Conrad, J. Jung, R. S. Penning, and M. R. Zinn, "Interleaved continuum-rigid manipulation: An augmented approach for robotic minimally-invasive flexible catheter-based procedures," in *Proc. 2013 IEEE Int. Conf. Robot. Automat. (ICRA)*. IEEE, 2013, pp. 718–724.

[63] T. Vandebroek *et al.*, "Macro-micro multi-arm robot for single-port access surgery," in *Proc. 2019 IEEE/RSJ Int. Conf. Intell. Robots Syst. (IROS)*. IEEE, 2019, pp. 425–432.

[64] C. Wang, Z. Li, Y. Ren, Y. Deng, and S. Song, "Design, control and analysis of a dual-arm continuum flexible robot system," in *Proc. 2019 IEEE Int. Conf. Robot. Biomimetics (ROBIO)*. IEEE, 2019, pp. 948–953.

[65] C. Zhang *et al.*, "Design optimization of pyramid-shaped transmission system for multiarm concentric-tube robots," *IEEE/ASME Trans. Mechatron.*, vol. 29, no. 5, pp. 3427–3438, 2024.

[66] C. Zhang *et al.*, "Design optimization of y-shaped transmission system for dual-arm concentric-tube robots," in *Proc. 2021 IEEE Int. Conf. Robot. Biomimetics (ROBIO)*. IEEE, 2021, pp. 571–576.

[67] Z. Mitros, S. H. Sadati, S. Nousias, L. Da Cruz, and C. Bergeles, "Design and quasistatic modelling of hybrid continuum multi-arm robots," in *Proc. 2022 IEEE Int. Conf. Robot. Automat. (ICRA)*. IEEE, 2022, pp. 9607–9613.

[68] J. Peng *et al.*, "Modeling, cooperative planning and compliant control of multi-arm space continuous robot for target manipulation," *Appl. Math. Model.*, vol. 121, pp. 690–713, 2023.

[69] Y. Dai, Z. Li, X. Chen, X. Wang, and H. Yuan, "A novel space robot with triple cable-driven continuum arms for space grasping," *Micromachines*, vol. 14, no. 2, 2023, Art. no. 416.

[70] J. Huang *et al.*, "Autologous variable stiffness soft finger based on cross-layer jamming for multimode grasping," *IEEE Robot. Autom. Lett.*, vol. 10, no. 2, pp. 1178–1185, 2024.

[71] G. Bolanakis and E. Papadopoulos, "Introducing mag-nets: Rapidly bending electromagnetic actuators for self-contained soft robots," *IEEE Robot. Autom. Lett.*, vol. 9, no. 6, pp. 5306–5313, 2024.

[72] Y. Zhang *et al.*, "Enhanced automated cell micromanipulation via programmable magnetic microgripper design," *IEEE Trans. Automat. Sci. Eng.*, vol. 22, pp. 10107–10117, 2024.

[73] A. Al-Ibadi, S. Nefti-Meziani, and S. Davis, "Cooperative project by self-bending continuum arms," in *Proc. 2017 IEEE 23rd Int. Conf. Autom. Comput. (ICAC)*. IEEE, 2017, pp. 1–6.

[74] C. Lu *et al.*, "Dexitac: Soft dexterous tactile gripping," *IEEE/ASME Trans. Mechatron.*, vol. 30, no. 1, pp. 333–344, 2024.

[75] M. G. Atia, A. Mohammad, A. Gameros, D. Axinte, and I. Wright, "Reconfigurable soft robots by building blocks," *Adv. Sci.*, vol. 9, no. 33, 2022, Art. no. 2203217.

[76] F. Hu and C. Zhang, "Origami polyhedra-based soft multicellular robots," *Soft Robot.*, vol. 11, no. 2, pp. 244–259, 2024.

[77] Q. Hu, Z. Chen, E. Dong, and D. Sun, "Design and control of a modular, untethered soft origami robot driven by sma coils," *IEEE Trans. Ind. Electron.*, vol. 72, no. 8, pp. 8208–8218, 2025.

[78] H. Wang *et al.*, "Design of a reconfigurable gripper with rigid-flexible variable fingers," *IEEE/ASME Trans. Mechatron.*, vol. 30, no. 1, pp. 505–516, 2024.

[79] H. Zhang, K. H. Heung, G. J. Naquila, A. Hingwe, and A. D. Deshpande, "A novel parameter estimation method for pneumatic soft hand control applying logarithmic decrement for pseudo-rigid body modeling," *Adv. Intell. Syst.*, vol. 7, no. 3, 2025, Art. no. 2400637.

[80] R. Zhen, L. Jiang, H. Li, and B. Yang, "Modular bioinspired hand with multijoint rigid-soft finger possessing proprioception," *Soft Robot.*, vol. 10, no. 2, pp. 380–394, 2023.

[81] J. Zhou, J. Huang, Q. Dou, P. Abeel, and Y. Liu, "A dexterous and compliant (dexco) hand based on soft hydraulic actuation for human inspired fine in-hand manipulation," *IEEE Trans. Robot.*, vol. 41, pp. 666–686, 2024.

[82] Q. Xia *et al.*, "An omnidirectional encircled deployable polyhedral gripper for contactless delicate midwater creatures sampling," *Adv. Eng. Mater.*, vol. 25, no. 8, 2023, Art. no. 2201416.

[83] D. Chu *et al.*, "Human palm performance evaluation and the palm design of humanoid robotic hands," *IEEE Robot. Autom. Lett.*, vol. 9, no. 3, pp. 2463–2470, 2024.

[84] Y. Ma *et al.*, "Comprehensive performance optimization of a novel anthropomorphic dexterous hand," *IEEE Robot. Autom. Lett.*, vol. 10, no. 7, pp. 6816–6823, 2025.

[85] T. Yue *et al.*, "Embodying soft robots with octopus-inspired hierarchical suction intelligence," *Sci. Robot.*, vol. 10, no. 102, 2025, Art. no. ead4264.

[86] X. Guo *et al.*, "Powerful uav manipulation via bioinspired self-adaptive soft self-contained gripper," *Sci. Adv.*, vol. 10, no. 19, 2024, Art. no. eadn6642.

[87] A. Jalali and F. Janabi-Sharifi, "Aerial continuum manipulation: A new platform for compliant aerial manipulation," *Front. Robot. AI*, vol. 9, 2022, Art. no. 903877.

[88] T. Mulu Girmay *et al.*, "Dynamic modeling of cooperative planar bionic manipulator," in *Proc. Mach. Mech. Robot.: Proc. iNaCoMM 2017*. Springer, 2018, pp. 839–849.

[89] S. Yang *et al.*, "Dynamic capture using a traplike soft gripper with stiffness anisotropy," *IEEE/ASME Trans. Mechatron.*, vol. 28, no. 3, pp. 1337–1346, 2022.

[90] J. Ye, J. Wang, B. Huang, Y. Qin, and X. Wang, "Learning continuous grasping function with dexterous hand from human demonstrations," *IEEE Robot. Autom. Lett.*, vol. 8, no. 5, pp. 2882–2889, 2023.

[91] H. Zhang *et al.*, "Adg-net: A sim2real multimodal learning framework for adaptive dexterous grasping," *IEEE Trans. Cybern.*, vol. 55, no. 2, pp. 840–853, 2025.

[92] C. Ye, Z. Liu, S. Yu, Z. Fan, and Y. Wang, "Design and motion analysis of a soft-limb robot inspired by bacterial flagella," *Biomimetics*, vol. 8, no. 3, 2023, Art. no. 271.

[93] Q. Ji *et al.*, "Synthesizing the optimal gait of a quadruped robot with soft actuators using deep reinforcement learning," *Robot. Comput. Manuf.*, vol. 78, 2022, Art. no. 102382.

[94] F. Fang *et al.*, "Hierarchically reconfigurable soft robots with reprogrammable multimodal actuation," *Adv. Funct. Mater.*, vol. 35, no. 4, 2025, Art. no. 2414279.

[95] D. Drotman, S. Jadhav, D. Sharp, C. Chan, and M. T. Tolley, "Electronics-free pneumatic circuits for controlling soft-legged robots," *Sci. Robot.*, vol. 6, no. 51, 2021, Art. no. eaay2627.

[96] M. Cianchetti, M. Calisti, L. Margheri, M. Kuba, and C. Laschi, "Bioinspired locomotion and grasping in water: the soft eight-arm octopus robot," *Bioinspir. Biomim.*, vol. 10, no. 3, 2015, Art. no. 035003.

[97] Z. J. Patterson, D. K. Patel, S. Bergbreiter, L. Yao, and C. Majidi, "A method for 3d printing and rapid prototyping of fieldable untethered soft robots," *Soft Robot.*, vol. 10, no. 2, pp. 292–300, 2023.

[98] R. Desatnik *et al.*, "Soft robotics informs how an early echinoderm moved," *Proc. Natl. Acad. Sci.*, vol. 120, no. 46, 2023, Art. no. e2306580120.

[99] S. Norouzi-Ghazbi and F. Janabi-Sharifi, "A switching image-based visual servoing method for cooperative continuum robots," *J. Intell. Robot. Syst.*, vol. 103, no. 3, 2021, Art. no. 42.

[100] Q. Wei *et al.*, "Collaborative control of space flexible multi-arm robot exploiting stress stiffening effect," *IEEE Trans. Aerosp. Electron. Syst.*, vol. 61, no. 1, pp. 1048–1065, 2024.

[101] Z. Qiao *et al.*, "Engineering a multi-stiffness nested cooperative magnetic continuum robot based on low melting point alloy," *Sci. China Technol. Sci.*, vol. 68, no. 8, 2025, Art. no. 1820301.

[102] M. Diezinger, B. Tamadazte, and G. J. Laurent, "Trirod: a 3-rf continuum parallel robot for shape-based load estimation," *IEEE Robot. Autom. Lett.*, vol. 8, no. 11, pp. 7265–7272, 2023.

[103] C. Nwafor, G. J. Laurent, and K. Rabenorosoa, "Miniature parallel continuum robot made of glass: Analysis, design, and proof-of-concept," *IEEE/ASME Trans. Mechatron.*, vol. 28, no. 4, pp. 2038–2046, 2023.

[104] X. Duan, W. Yan, T. Yan, G. Chen, and H. Wang, "Kinematics modeling and analysis of a spherical parallel continuum manipulator," *J. Mech. Robot.*, vol. 17, no. 1, 2025, Art. no. 011004.

[105] X. Huang, X. Zhu, and G. Gu, "Kinematic modeling and characterization of soft parallel robots," *IEEE Trans. Robot.*, vol. 38, no. 6, pp. 3792–3806, 2022.

[106] K. Wen and J. Burgner-Kahrs, "Modeling and analysis of tendon-driven parallel continuum robots under constant curvature and pseudo-rigid-body assumptions," *J. Mech. Robot.*, vol. 15, no. 4, 2023, Art. no. 041003.

[107] K. Nuelle *et al.*, "Modeling, calibration, and evaluation of a tendon-actuated planar parallel continuum robot," *IEEE Robot. Autom. Lett.*, vol. 5, no. 4, pp. 5811–5818, 2020.

[108] P. Yu, N. Tan, Y. Wu, B. Qiu, and K. Huang, "Model-free synchronous motion generation of multiple heterogeneous continuum robots," *IEEE Trans. Ind. Inf.*, vol. 20, no. 3, pp. 3209–3221, 2023.

[109] N. Tan *et al.*, "Synchronous motion generation of multiple continuum robots based on a jacobian-estimation strategy," in *Proc. 2021 IEEE Int. Conf. Robot. Biomimetics (RIBIO)*. IEEE, 2021, pp. 475–482.

[110] M. C. Lastinger, A. Rice, A. Kapadia, and I. D. Walker, "Variable topology "tree-like" continuum robots for remote inspection and cleaning," in *Proc. 2020 IEEE Aerosp. Conf.* IEEE, 2020, pp. 1–10.

[111] A. Lotfavar, S. Hasanzadeh, and F. Janabi-Sharifi, "Cooperative continuum robots: Concept, modeling, and workspace analysis," *IEEE Robot. Autom. Lett.*, vol. 3, no. 1, pp. 426–433, 2017.

[112] A. Jalali and F. Janabi-Sharifi, "Dynamic modeling of tendon-driven co-manipulative continuum robots," *IEEE Robot. Autom. Lett.*, vol. 7, no. 2, pp. 1643–1650, 2021.

[113] S. Lilge and J. Burgner-Kahrs, "Kinematic modeling of tendon-driven parallel continuum robots," *IEEE Trans. Robot.*, vol. 39, no. 2, pp. 1563–1579, 2022.

[114] P. L. Anderson, A. W. Mahoney, and R. J. Webster, "Continuum reconfigurable parallel robots for surgery: Shape sensing and state estimation with uncertainty," *IEEE Robot. Autom. Lett.*, vol. 2, no. 3, pp. 1617–1624, 2017.

[115] X. Li *et al.*, "Design and modeling of a multi-backbone continuum robot with a large extension ratio," *Mech. Mach. Theory*, vol. 206, 2025, Art. no. 105935.

[116] M. Tummers *et al.*, "Cosserat rod modeling of continuum robots from newtonian and lagrangian perspectives," *IEEE Trans. Robot.*, vol. 39, no. 3, pp. 2360–2378, 2023.

[117] A. Mehrkish and F. Janabi-Sharifi, "Grasp synthesis of continuum robots," *Mech. Mach. Theory*, vol. 168, 2022, Art. no. 104575.

[118] X. Wang, H. Kuang, C. Zhu, and K. Xu, "Closed-loop cooperative manipulation of deformable tissue via visual feedback using multiple continuum surgical manipulators," *IEEE Robot. Autom. Lett.*, vol. 10, no. 5, pp. 4396–4403, 2025.

[119] B. Su *et al.*, "Cooperative position and attitude following between master and slave continuum robots," in *Proc. 2022 IEEE WRC Symp. Adv. Robot. Autom. (WRC SARA)*. IEEE, 2022, pp. 89–94.

[120] Z. Chen *et al.*, "Data-driven methods applied to soft robot modeling and control: A review," *IEEE Trans. Automat. Sci. Eng.*, vol. 22, pp. 2241–2256, 2024.

[121] H. J. Zhang, S. Lilge, M. T. Chikhaoui, and J. Burgner-Kahrs, "Cooperative control of dual-arm concentric tube continuum robots," in *Proc. 2022 Int. Conf. Manip. Autom. Robot. Small Scales (MARSS)*. IEEE, 2022, pp. 1–6.

[122] Y. Hu, W. Li, L. Zhang, and G.-Z. Yang, "Designing, prototyping, and testing a flexible suturing robot for transanal endoscopic microsurgery," *IEEE Robot. Autom. Lett.*, vol. 4, no. 2, pp. 1669–1675, 2019.

[123] A. Mehrkish, F. Janabi-Sharifi, M. Goharimanesh, and S. Norouzi-Ghazbi, "Multiple aspects grasp quality evaluation in underactuated grasp of tendon-driven continuum robots," *Int. Serv. Robot.*, vol. 16, no. 1, pp. 33–48, 2023.

[124] F. Wang *et al.*, "Research on variable workspace of continuum robot for organ protection and multi-arm cooperation," in *Proc. 2022 12th IEEE Int. Conf. CYBER Technol. Autom. Control Intell. Syst. (CYBER)*. IEEE, 2022, pp. 978–982.

[125] S. Sabetian, T. Looi, E. D. Diller, and J. Drake, "Self-collision detection and avoidance for dual-arm concentric tube robots," *IEEE Robot. Autom. Lett.*, early access, Aug. 2019.

[126] A. Kuntz *et al.*, "Motion planning for continuum reconfigurable incisionless surgical parallel robots," in *Proc. 2017 IEEE/RSJ Int. Conf. Intell. Robots Syst. (IROS)*. IEEE, 2017, pp. 6463–6469.

[127] M. F. Rox *et al.*, "Mechatronic design of a two-arm concentric tube robot system for rigid neuroendoscopy," *IEEE/ASME Trans. Mechatron.*, vol. 25, no. 3, pp. 1432–1443, 2020.

[128] K. Xu, J. Zhao, and M. Fu, "Development of the sjtu unfoldable robotic system (surs) for single port laparoscopy," *IEEE/ASME Trans. Mechatron.*, vol. 20, no. 5, pp. 2133–2145, 2014.

[129] C. Li, X. Gu, X. Xiao, C. M. Lim, and H. Ren, "Cadaveric feasibility study of a teleoperated parallel continuum robot with variable stiffness for transoral surgery," *Med. Biol. Eng. Comput.*, vol. 58, no. 9, pp. 2063–2069, 2020.

[130] J. Liu *et al.*, "Data-driven methods for sensing, modeling and control of soft continuum robot: A review," *IEEE/ASME Trans. Mechatron.*, early access, May 2025.

[131] S. Song, H. Ge, J. Wang, and M. Q.-H. Meng, "Real-time multi-object magnetic tracking for multi-arm continuum robots," *IEEE Trans. Instrum. Meas.*, vol. 70, pp. 1–9, 2021.

[132] B. Wu, L. Wang, X. Liu, L. Wang, and K. Xu, "Closed-loop pose control and automated suturing of continuum surgical manipulators with customized wrist markers under stereo vision," *IEEE Robot. Autom. Lett.*, vol. 6, no. 4, pp. 7137–7144, 2021.

[133] H. Yang, B. Wu, X. Liu, and K. Xu, "A closed-loop controller for a continuum surgical manipulator based on a specially designed wrist marker and stereo tracking," in *Proc. 2020 IEEE/ASME Int. Conf. Adv. Intell. Mechatron. (AIM)*. IEEE, 2020, pp. 335–340.

[134] K. Xu *et al.*, "System design of an insertable robotic effector platform for single port access (spa) surgery," in *Proc. 2009 IEEE/RSJ Int. Conf. Intell. Robots Syst. (IROS)*. IEEE, 2009, pp. 5546–5552.

[135] A. Reiter *et al.*, "A learning algorithm for visual pose estimation of continuum robots," in *Proc. 2011 IEEE/RSJ Int. Conf. Intell. Robots Syst. (IROS)*. IEEE, 2011, pp. 2390–2396.

[136] L. Wang, C. Zhou, Y. Cao, R. Zhao, and K. Xu, "Vision-based markerless tracking for continuum surgical instruments in robot-assisted minimally invasive surgery," *IEEE Robot. Autom. Lett.*, vol. 8, no. 11, pp. 7202–7209, 2023.

[137] C. Zhou, L. Wang, B. Wu, and K. Xu, "A markerless 3d tracking framework for continuum surgical tools using a surgical tool partial pose estimation network based on domain randomization," *Adv. Intell. Syst.*, vol. 6, no. 4, 2024, Art. no. 2300434.

[138] H. Guo *et al.*, "Multi-continuum manipulators shape reconstruction using inertial navigation sensors and cameras," *Ind. Robot.*, vol. 48, no. 3, pp. 401–412, 2021.

[139] S. Lilge, T. D. Barfoot, and J. Burgner-Kahrs, "State estimation for continuum multi-robot systems on se (3)," *IEEE Trans. Robot.*, vol. 41, pp. 905–925, 2024.

[140] J. C. Tejada, T.-O. Alejandro, A. López-Gonzalez, E. G. Hernandez-Martinez, and D. Sanin-Villa, "A review of multi-robot systems and soft robotics: Challenges and opportunities," *Sen.*, vol. 25, no. 2, 2025, Art. no. 1353.

[141] A. Miele, M. Lippi, and A. Gasparri, "A distributed framework for integrated task allocation and safe coordination in networked multi-robot systems," *IEEE Trans. Autom. Sci. Eng.*, vol. 22, pp. 11219–11238, 2025.

[142] J. Zhao, Y. Huang, J. Feng, W. Xie, and K. Jain, "Fusion of kano theory and attention-bilstm models for user demand analysis and trend prediction," *Inf. Fusion.*, 2025, Art. no. 103210.

[143] S. Jiang, W. Li, Y. Qian, Y. Zhang, and J. Luo, "Autotriz: Automating engineering innovation with triz and large language models," *Adv. Eng. Inform.*, vol. 65, 2025, Art. no. 103312.

[144] M. Ghane *et al.*, "Semantic triz feasibility in technology development, innovation, and production: A systematic review," *Helion*, vol. 10, no. 1, 2024, Art. no. e23775.

[145] M. Raissi, P. Perdikaris, and G. E. Karniadakis, "Physics-informed neural networks: A deep learning framework for solving forward and inverse problems involving nonlinear partial differential equations," *J. Comput. Phys.*, vol. 378, pp. 686–707, 2019.

[146] M. Bensch, T.-D. Job, T.-L. Habich, T. Seel, and M. Schappler, "Physics-informed neural networks for continuum robots: Towards fast approximation of static cosserat rod theory," in *Proc. 2024 IEEE Int. Conf. Robot. Automat. (ICRA)*. IEEE, 2024, pp. 17293–17299.

[147] T. George Thuruthel, Y. Ansari, E. Falotico, and C. Laschi, "Control strategies for soft robotic manipulators: A survey," *Soft Robot.*, vol. 5, no. 2, pp. 149–163, 2018.

[148] M. Lai *et al.*, "Roboballet: Planning for multirobot reaching with graph neural networks and reinforcement learning," *Sci. Robot.*, vol. 10, no. 106, 2025, Art. no. eads1204.

[149] F. Yang *et al.*, "Task-oriented tool manipulation with robotic dexterous hands: A knowledge graph approach from fingers to functionality," *IEEE Trans. Cybern.*, vol. 55, no. 1, pp. 395–408, 2024.

[150] B. Li *et al.*, "Interactive learning for multi-finger dexterous hand: A model-free hierarchical deep reinforcement learning approach," *Knowledge-based Syst.*, vol. 295, 2024, Art. no. 111847.

[151] Y. Chen *et al.*, "Bi-dexhands: Towards human-level bimanual dexterous manipulation," *IEEE Trans. Pattern Anal. Machine Intell.*, vol. 46, no. 5, pp. 2804–2818, 2023.

[152] J. A. Barreiros *et al.*, "Learning contact-rich whole-body manipulation with example-guided reinforcement learning," *Sci. Robot.*, vol. 10, no. 105, 2025, Art. no. eads6790.

[153] X. Huo, H. Zhang, Z. Wang, C. Huang, and H. Yan, "A self-learning approach to heterogeneous multi-robot coalition formation under uncertainty," *IEEE Trans. Automat. Sci. Eng.*, vol. 22, pp. 3445–3457, 2024.

[154] Y. Miao, X. Liu, S. Yang, and J. Ma, "Fabrication of self-sensing soft robots via multi-material digital light processing 3d printing of hydrogels," *Mater. Des.*, 2025, Art. no. 114394.

[155] B. Kang *et al.*, "A flexible skin-mounted haptic interface for multimodal cutaneous feedback," *Nat. Electron.*, early access, Jun. 2025.

[156] Y. Wang, W. Wang, and G. Bao, "Design and control scheme of a rigid-flexible coupled duel-arm hug robots," in *Proc. 2024 IEEE-RAS 23rd Int. Conf. Humanoid Robots (Humanoids)*. IEEE, 2024, pp. 1027–1033.

[157] M. Shiomi, A. Nakata, M. Kanbara, and N. Hagita, "A hug from a robot encourages prosocial behavior," in *Proc. 2017 26th IEEE Int. Symp. Robot Human Interact. Commun. (RO-MAN)*. IEEE, 2017, pp. 418–423.

[158] A. Sebastian, "Soft robotics for search and rescue: Advancements, challenges, and future directions," *arXiv preprint arXiv:2502.12373*, 2025.

[159] R. Peng, Y. Wang, M. Lu, and P. Lu, "A dexterous and compliant aerial continuum manipulator for cluttered and constrained environments," *Nat. Commun.*, vol. 16, no. 1, 2025, Art. no. 889.

[160] C. Armanini *et al.*, "Soft robotics for farm to fork: applications in agriculture & farming," *Bioinspir. Biomim.*, vol. 19, no. 2, 2024, Art. no. 021002.

[161] K. Lochan *et al.*, "Advancements in precision spraying of agricultural robots: A comprehensive review," *IEEE Access*, vol. 12, pp. 129447–129483, 2024.